universität wien

# DIPLOMARBEIT / DIPLOMA THESIS

Titel der Diplomarbeit / Title of the Diploma Thesis

„Generation of clonal cell lines from fibroblasts of female RETT syndrome patients“


verfasst von / submitted by

Melanie Rebecka Olczykowski


angestrebter akademischer Grad / in partial fulfilment of the requirements for the degree of

Magistra der Pharmazie (Mag.pharm.)

Wien, 2021 / Vienna, 2021

| | |
|---|---|
| Studienkennzahl lt. Studienblatt / degree programme code as it appears on the student record sheet: | A 449 |
| Studienrichtung lt. Studienblatt / degree programme as it appears on the student record sheet: | Diplomstudium Pharmazie |
| Betreut von / Supervisor: | Univ.-Prof. Dipl.-Ing. Dr. Manfred Ogris |

*First of all, I would like to thank my family and friends for their endless support and encouragement during my studies. The biggest thank you goes to my mum and my brother who always had my back no matter what.*

*I would also like to thank the Laccone Research group at the Medical University of Vienna, especially Prof. Dr. Franco Laccone and Dr. Hannes Steinkellner, for giving me the opportunity to get an insight into research and for guiding me throughout the time of experiments.*

*And lastly, thank you to my guardian angel, dearly father, who I know is always watching and keeping an eye on me.*

# Table of contents


1. Abstract ..... 8
2. Zusammenfassung ..... 9
3. List of figures ..... 10
4. Introduction ..... 11
   - 4.1. Rett Syndrome ..... 11
   - 4.2. Phenotype ..... 11
   - 4.3. Mutation of the MECP2 Gene ..... 13
   - 4.4. MeCP2 Structure ..... 14
   - 4.5. MeCP2 in a Mouse Model ..... 17
   - 4.6. Hyperacetylation ..... 18
   - 4.7. Inheritance of Rett Syndrome ..... 19
   - 4.8. Diagnosis & Therapeutic strategies ..... 19
   - 4.9. Single-Cell isolation techniques ..... 22
     - 4.9.1. Cell sorting by Flow Cytometry (FC) ..... 23
     - 4.9.2. QIAscout™ ..... 23
     - 4.9.3. Limiting Dilution Cloning ..... 24
5. Aims of the thesis ..... 25
6. Materials and Methods ..... 26
   - 6.1. Reagents ..... 26
   - 6.2. Solutions and buffers ..... 28
     - TBE buffer (10x), pH= 8.3 ..... 28
     - PBS (10x), pH = 7.4 ..... 28
     - Tris-HCl (1M, pH = 6.8) ..... 28
     - PBST (PBS + 0.05% Tween 20) ..... 29
     - Electrophoresis Buffer ..... 29
     - Tris-Tricine (10x) Buffer ..... 29
     - Blotting Buffer ..... 29
     - Tris-Glycine (10x) Buffer ..... 30
   - 6.3. Materials ..... 30
   - 6.4. Technical equipment ..... 31
   - 6.5. Cell lines ..... 31
     - 6.5.1. Morphology of cell lines ..... 33
   - 6.6. Cell culture ..... 33
     - 6.6.1. Thawing of cell lines ..... 33
     - 6.6.2. Cell splitting ..... 34
     - 6.6.3. Changing of Cell Culture Medium ..... 34
     - 6.6.4. Preparation of Conditioned Medium ..... 34

6.6.5. Cell freezing ..... 34
6.6.6. Karyotyping ..... 35
6.7. Single cell Isolation Methods ..... 35
6.7.1. Cell sorting (FC) ..... 35
6.7.2. Limiting Dilution Cloning ..... 36
6.7.3. QIAscout™ ..... 36
6.8. Genotyping ..... 37
6.8.1. DNA Extraction ..... 37
6.8.2. Human Androgen Receptor Assay (HUMARA Assay) ..... 38
6.8.3. RNA Extraction ..... 39
6.8.4. Reverse Transcription of RNA to cDNA ..... 39
6.8.5. Preparation of cDNA from clonal cells for further sequencing ..... 40
6.8.5.1. 2% Agarose Gel Electrophoresis ..... 42
6.9. Immunofluorescence (IF) ..... 42
6.10. NEON Transfection ..... 43
6.11. Western Blot ..... 44
6.11.1. Sample Preparation ..... 44
6.11.2. Gel Electrophoresis ..... 44
6.11.3. Transfer ..... 44
6.11.4. Blocking ..... 44
6.11.5. Antibody Incubation ..... 45
7. Results ..... 46
7.1. Karyotyping ..... 46
7.2. Comparison of methods for single cell seeding ..... 47
7.2.1. Limiting Dilution Cloning ..... 47
7.2.2. QIAscout™ ..... 48
7.2.3. Cell sorting by Flow Cytometry (FC) ..... 48
7.3. Seedings ..... 49
7.4. Determination of the genotype of the c705delG cell line ..... 53
7.4.1. Confirmation of monoclonal cells by HUMARA Assay ..... 53
7.4.2. Verifying of clonal cells by Immunofluorescence ..... 53
7.5. Determination of the genotype of the T158M cell line ..... 56
7.5.1. Confirmation of the presence of MeCP2 positive cells by sequencing ..... 56
7.6. Acetylation status of RETT monoclonal cells ..... 57
8. Discussion ..... 59
8.1. Single cell isolation ..... 59
8.2. Treatment of single cells ..... 60
8.3. Identification of clones ..... 61
8.4. Hyperacetylation in RTT ..... 62
8.5. Conclusion ..... 62

9. Appendix ..... 64
9.1. Results of the HUMARA Assay before and after digestion ..... 64
9.1.1. Clone A ..... 64
9.1.2. Clone B ..... 65
9.1.3. Clone C ..... 66
9.1.4. c705delG ..... 67
9.1.5. Male control cells ..... 68
10. References ..... 69

# 1. Abstract

Mutations in the methyl-CpG-binding protein 2 (*MECP2*) gene which encodes the protein MeCP2, a crucial modulator of gene expression, are the main cause of Rett Syndrome (RTT), an X-linked neurodevelopmental disorder that appears in children. In order to advance the development of therapies for RTT, the need to establish the appropriate cell models is apparent.

It is hence the aim of this work to isolate single cells from a Rett patient's fibroblasts and ultimately obtain monoclonal cells such as mutant and wildtype MeCP2 clones. For this purpose, three different methods were used and compared: Flow cytometry (FC), limiting dilution cloning and QIAscout™. Numerous seedings were performed; clones were treated with various mediums, cells were immortalized and transfected with the plasmid pCl neo-hEST2 via electroporation. Clones were obtained and then characterized by immunofluorescence staining, the HUMARA assay and Sanger sequencing. Results showed a difference between different treatments of clones as well as cells that were treated with and without plasmid. Lastly, the status of histone hyperacetylation in monoclonal cells, which is essential in RTT, was determined by western blot with an antibody directed against acetylated histone H3 at Lys9 (H3k9).

In summary, we have developed a cellular model for Rett Syndrome by using single cell-derived wild-type and mutant MECP2 expressing fibroblast clones with a common mutation in MeCP2 (705delG). Furthermore, we were able to demonstrate a RETT-specific phenotype in this model by investigating the hyperacetylation status and therefore it could serve as a cell model for high throughput screening of therapeutic agents, diagnosis and personalized treatment.

# 2. Zusammenfassung

Das Rett Syndrom (RTT) ist eine X-chromosomale neurologische Entwicklungsstörung, die bei Kindern auftritt. Die Hauptursachen für diese Erkrankung sind Mutationen im Methyl-CpG-Bindungsprotein 2 (*MECP2*) Gen, welches für das Protein MeCP2 codiert und als entscheidender Modulator der Genexpression fungiert. Um die Entwicklung von Therapien für RTT voranzutreiben ist es notwendig, geeignete Zellmodelle zu etablieren.

Das Ziel dieser Arbeit ist es daher, einzelne Zellklone aus den Fibroblasten eines Rett-Patienten zu isolieren und dadurch monoklonale Zellen von mutiertem und Wildtyp MeCP2 zu erhalten. Zu diesem Zweck wurden drei verschiedene Methoden verwendet und verglichen: Durchflusszytometrie, Limiting Dilution Cloning und QIAscout™. Es wurden zahlreiche Vereinzelungen durchgeführt; Klone wurden mit verschiedenen Medien behandelt, die Zellen wurden immortalisiert und mittels Elektroporation mit dem Plasmid pCl neo-hEST2 transfiziert. Nach Erhalt der Klone wurden diese dann durch Immunfluoreszenzfärbung, HUMARA-Assay und Sanger-Sequenzierung charakterisiert. Die Ergebnisse zeigten einen Unterschied hinsichtlich verschiedener Behandlungen von Klonen sowie Zellen, die mit und ohne Plasmid behandelt wurden. Schließlich wurde der Status der Histonacetylierung in monoklonalen Zellen, der wesentlich beim RTT ist, mittels Western Blot mit einem gegen acetylisiertes Histon H3 bei Lys9 (H3k9) gerichteten Antikörper bestimmt.

Zusammenfassend haben wir ein zelluläres Modell für das Rett-Syndrom entwickelt, bei dem aus Einzelzellen stammende Wildtyp- und mutierte MeCP2-exprimierende Fibroblastenklone mit einer häufigen Mutation in MeCP2 (705delG) verwendet wurden. Darüber hinaus konnten wir in diesem Modell einen RETT-spezifischen Phänotyp zeigen, in dem wir den Hyperacetylierungsstatus untersuchten. Dieses Zellmodell könnte für das Hochdurchsatz-Screening von Therapeutika, sowie der Diagnostik und der personalisierten Behandlung dienen.

# 3. List of figures

**Figure 1** Structure of the *MECP2* gene. ..... 15
**Figure 2** Targets and treatment strategies..... 21
**Figure 3** Microscope images of human fibroblast Rett syndrome cells……...33
**Figure 4** Results of Karyotyping……..46
**Figure 5** QIAscout array..... 48
**Figure 6** Development of QIAscout seeding. ..... 50
**Figure 7** Timeline of cell cloning from day one until moving first clone……52
**Figure 8** IF images showing non transfected c705delG cells treated with and without G418.53
**Figure 9** Immunofluorescence images from two control cell lines at 20x magnification..... 54
**Figure 10** Immunofluorescence images from obtained clones at 20x magnification..... 55
**Figure 11** Cell lines incubated with the MeCP2 XP antibody ..... 56
**Figure 12** PCR that was performed with the cells of the mutation T158M ..... 57
**Figure 13** Results of sequencing ..... 57
**Figure 14** Analysis of acetylation status of monoclonal cells ..... 58

# 4. Introduction

## 4.1. Rett Syndrome

Rett syndrome (RTT) a neurodevelopmental disorder, was first discovered in 1966 by the Austrian pediatrician Andreas Rett. After observing two little kids in the waiting room of his office, he first noticed the identical hand movements called “washing hands”. As the clinical and developmental history of the girls was very similar, he decided to travel through Europe and look for other children with the same significant symptoms. He was the first to describe 22 cases of young female patients who all shared these identical symptoms (Leonard et al., 2016).

## 4.2. Phenotype

The development of the children appears progressively in four stages:

- Stagnation (age 6–18 months)
- Rapid regression (age 1–4 years)
- Pseudostationary/ Plateau period (age 2–potentially life)
- Late motor deterioration (age 10–life)

First, postnatal development is normal. Most kids even learn how to walk or speak, while others already display stagnant development. RTT symptoms usually arise between 6 to 18 months of age. After 18 months the development arrests and is followed by a rapid regression. In this phase, it is common for children to be missing developmental milestones and losing cognitive-, motor- and communication skills that have been previously gained (Kyle et al., 2018).

RTT onset is strongly associated with mutations in the *MECP2* gene which encodes the protein MeCP2, a crucial modulator of gene expression (Shah & Bird, 2017). A loss of MeCP2 disturbs the region or system in the brain from which it is deleted, because normally it plays a crucial role in brain development and function (Leonard et al., 2016).

Symptoms often include:

- Problems in motoric function like unintentional hand movements such as hand washing or complete loss of purposeful use of hands
- Loss of speech
- Slow growth
- Loss of mobility or gait abnormalities
- Loss of muscle tone
- Scoliosis
- Problems breathing
- Sleep disorders
- Seizures or Rett "Episodes"
- Cardiac issues
- Swallowing and digestion abnormalities
- Autistic characteristics
- Microcephaly

(What Is Rett Syndrome, www.rettsyndrome.org)

As patients get older, they can partly regain some of their skills lost during the regression period, but a significant loss of verbal skills and purposeful hand use continues to be a hallmark of the disorder (Kaufmann et al., 2016). There is an expectation that besides any complications or illnesses patients normally survive into adulthood. Following data from the Natural History Study shows different chances of a girl with Rett syndrome reaching a specific age:

***Table 1.*** *Chances of survival of girls with Rett syndrome* (What Is Rett Syndrome, www.rettsyndrome.org)

| | |
|---|---|
| 100% chance | of reaching the age 10 |
| 90% chance | of reaching the age 20 |
| 75% chance | of reaching the age 30 |
| 65% chance | of reaching the age 40 |
| 50% chance | of reaching the age 50 |

RTT patients have a high incidence of sudden unpredictable deaths (26% of all RTT associated deaths) which may be caused by cardiac dysfunction such as long-QT-syndrome.

The cause for a prolonged long-QT-interval in RTT patients is still unknown and untested (McCauley et al., 2011).
In addition, due to mostly the same phenotypes and the social withdrawal and social interactions, Rett patients are often misdiagnosed as autistic patients (Liyanage & Rastegar, 2014).

However, not all *MECP2* mutations cause RTT but rather a mild intellectual disability (Ehrhart et al., 2016). When a child does not fulfill the diagnostic criteria for RTT but shows RTT-like symptoms, then they may be diagnosed with atypical RTT which for example show mutations in two other genes, in the x-linked cyclin - dependent kinase 5 (CDKL5) or in the Forkhead box protein G1 (FOXG1). Nonetheless, some other mutations still remain undefined (Kyle et al., 2018).

Currently, the incidence of RTT is 1 in 15.000 live births, which translates to 3-5 affected girls in a year in Austria (Österreichische Rett-Syndrom Gesellschaft, www.rett-syndrom.at).
Along with the aforementioned symptoms, RTT leads to lifelong mental and physical disabilities, which do not allow to lead an independent lifestyle. Although affected individuals may retain some hand control or walking ability, typical hand stereotypes become prominent and constitute and most will be wheelchair-dependent and require on 24-hour care throughout their lives (Smeets et al., 2012).

## 4.3. Mutation of the *MECP2* Gene

RTT is the first human disease that is triggered by a malfunction in a protein that is involved in regulation of gene expression of thousands of other genes by interacting with methylated DNA. The disease is caused by mutations on the Methyl-CpG-binding protein 2 gene (*MECP2*) which occurs on the X chromosome at Xq28 (Webb & Latif, 2001). MeCP2 itself acts as a transcriptional repressor and global modulator in gene expression (Shah & Bird, 2017) and besides its distribution in different tissue types, it plays a particular role in the nervous system. Because of that, RTT is thought to result from a lack of functional protein in the brain (Chahrour et al., 2008; Steinkellner et al., 2019;).
RTT mainly affects females who possess two X chromosomes, which means that either one has a copy of the *MECP2* gene. Even if one X chromosome is affected by the mutation or has a change in the copy of the gene, another X chromosome supplies a wild type copy of the

gene (Shah & Bird, 2017). Therefore, X-inactivation is the reason that only one copy of the *MECP2* gene is active in any cell in female RTT patients. This means that those females have roughly one half of their cells that function normally and the other half of their cells have a *MECP2* gene with a mutation that does not (What Is Rett Syndrome, www.rettsyndrome.org). Thus, girls affected with RTT are somatic mosaics for cells that either express a wild type or a mutant version of the gene (Ross et al., 2016; Steinkellner et al., 2019;).

Males (which possess only one X chromosome) with a similar mutation tend to have severe congenital encephalopathies and rarely survive infancy and die during their first two years of life (Shah & Bird, 2017).

However, it has been found that most of spontaneous mutations in the *MECP2* gene occur during the division and formation of the sperm. That is the reason for the absence of the RTT in males. Since fathers give their X chromosome to their daughters and their Y chromosome to their sons, the chance for male RTT to emerge is very small.
Nonetheless, since testing of the *MECP2* gene has been available, there have been over 60 documented cases of males with *MECP2* mutations. A few of these males showed the same clinical picture meeting the criteria for diagnosing RTT, but most of them showed a different clinical presentation such as symptoms beginning at or shortly after birth (What Is Rett Syndrome, www.rettsyndrome.org).

Most patients were identified with mutations in the coding region of the *MECP2* gene. This includes point mutations like nonsense, missense and frameshifts. Others may have mutations in other regions of the gene, such as regulatory elements and noncoding regions (Buyse et al., 2000). In 60% of girls with classical RTT there were relatively frequent mutations found, which are all C → T transitions. Another 10% of mutations are small deletions, mainly in the C terminal region (Webb & Latif, 2001).

## 4.4. MeCP2 Structure

*MECP2* is a X-linked gene in the long arm of the X chromosome Xq28 [Figure 1]. It is located between the Interleukin-1 receptor associated kinase gene (IRAK1) and Red Opsin gene (RCP) and consists of four major exons and three introns. The resulting MeCP2 protein structure contains five major components: N-terminal Domain, Methyl-Binding Domain, Inter

Domain, Transcription Repression Domain and C-terminal Domain (Liyanage & Rastegar, 2014).

Two of these domains are most important for protein function: Methyl-CpG-binding domain (MBD) and transcriptional repression domain (TRD) (Ehrhart et al., 2016).
The MBD is 85 amino acids in length. It binds to CpG dinucleotides that are methylated at position 5 of the cytosine (5mC). Although the protein preferably binds to 5mC rich CpG island, it can also bind to any 5mC in the genome.
TRD is 104 amino acids in length and is responsible for recruiting the co-repressor Sin3A and the histone deacetylase, which consequentially results in transcriptional repression (Webb & Latif, 2001).

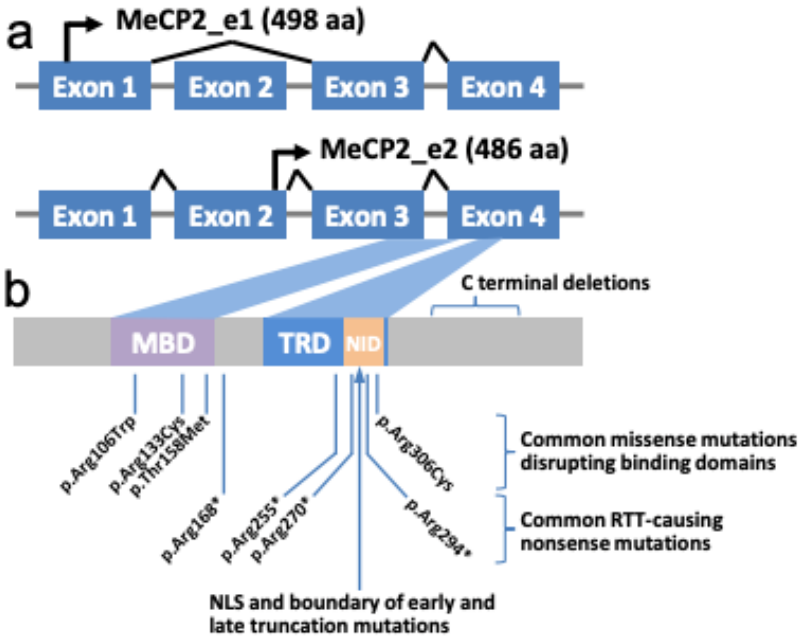


***Figure 1 a | b.*** *Structure of the MECP2 gene.* ***a*** *| The two mRNA isoforms, MECP2_e1 and MECP2_e2.* ***b*** *| The MeCP2 protein contains major domains that are relevant to Rett syndrome pathology: Methyl-CpG-binding domain (MBD), transcriptional repression domain (TRD) and NCOR-SM SMRT interaction domain (NID). Missense mutations mostly cluster around the MBD or TRD/NID region.* (Reprinted by permission from Springer Nature, Leonard et al., 2016, Clinical and biological progress over 50 years in Rett syndrome).

MBD and the TRD are the only structured domains (Ehrhart et al., 2016) while the rest of the protein (60%) is unstructured and considered as an intrinsically disordered protein (Liyanage & Rastegar, 2014).

As mentioned before, the *MECP2* gene consists of four exons and three introns. The transcriptional levels of exon 1 are much higher than of other exons in the brain and that is why mutations in the *MECP2* exon 1 are enough to cause RTT (Jin et al., 2017).
The coding sequence for the MBD is in between exons 3 and 4 while the TRD is located exclusively in exon 4. The 5'UTR lies in exon 1 and a part of exon 2, whereas the 3'UTR lies in exon 4 of the *MECP2* gene and contains several polyadenylated sites (Webb & Latif, 2001).

As mentioned, MeCP2 is a DNA binding protein that acts as a transcriptional repressor and inhibits the transcription of genes with methylated promoters after binding to methylated CpG dinucleotides through its methyl-binding domain. There are two ways in which this repression can be achieved. One such mechanism is hindering the methyl group from transcription factor binding. Second, indirect methylation of the promoter region prevents gene transcription by another protein that binds to methylated CpG (Webb & Latif, 2001).

It was also reported that MeCP2's transcriptional repressor activity includes the compaction and reorganization of chromatin (Nectoux et al., 2010). MeCP2 recruits a co-repressor named Sin3A and histone deacetylase into a complex after binding to the methylated CpG in the target DNA. In the nucleosomes, the complex deacetylates the tails of histones H3 and H4. Thus, deacetylation of histones leads to compaction of chromatin, which makes it inaccessible for transcription. By inhibiting histone deacetylase activity, silencing can be ameliorated (Webb & Latif, 2001).

However, MeCP2 can also act as an activator of transcription. Studies showed that MeCP2 associates with the transcriptional activator CREB1 at a promotor of an activated target. It suggests that MeCP2 regulates the expression of a large range of genes in the hypothalamus. Therefore, its function varies and can be both, an activator and repressor of transcription (Chahrour et al., 2008).

In addition, there are known two mRNA isoforms, *MECP2_e1* and *MECP2_e2* that generate two respective protein isoforms. The difference between those two isoforms is in the N-termini due to the use of two distinct translation start sites and the presence or absence of exon 2 in the transcript. MeCP2_e1 is the dominant isoform but both forms seem to be functionally identical with some minor variations (Leonard et al., 2016).

The expression of MeCP2 with cellular localization specifically in neurons but not in glia, is thought to be the highest in the brain. However, this protein is also present in the lung and spleen and to a lesser extent in the kidney and heart. That is why most symptoms of RTT are related to the central nervous system dysfunction (Traynor et al., 2002). In another study, reports of comparably high levels in the lung and heart were not confirmed, and it was demonstrated that the expression levels in the brain were much higher than in any other tested tissues (Ross et al., 2016).

## 4.5. MeCP2 in a Mouse Model

The amino acid sequence of MeCP2 has a 95% identity between humans and mice (Katz et al., 2016). While heterozygous female mice develop overt phenotypes at a much later developmental point than humans do, they still are the closest genetic representation of most patients with RTT (Leonard et al., 2016). Mutation or deletion studies in *Mecp2* of mice show that their phenotype is comparable but less severe than in humans with RTT (Luikenhuis et al., 2004).

These mice model experiments have been revealing that even late in disease progression, it is possible to improve symptoms of RTT (Kaufmann et al., 2016).

The impact of the total absence of MeCP2 was explored in several model systems. In a study of a mouse model with a specific deletion of *Mecp2* in the forebrain caused behavioral abnormalities as well as problems with motor coordination, anxiety and abnormal social behavior but not affecting locomotor activity or alterations in fear conditioning. Another mouse model study in which *Mecp2* was silenced in the GABAergic neurons, led to a very serious RTT-like phenotype (Ehrhart et al., 2016). The deletion of *Mecp2* from the glia in mice did not result in any significant phenotypic consequences, but restoration of MeCP2 in astrocytes led to partial improvement regarding motoric functions and breathing patterns phenotype. Overall, studies showed that a deficiency of MeCP2 in neurons is generally believed to be the primary culprit in RTT onset and the cause for RTT associated symptoms (Leonard et al., 2016). It was also found that by simultaneously modulating GABAergic and serotoninergic neurotransmission in mouse models, improvement in breathing patterns can be achieved. Nevertheless, it is still unknown whether this can be achieved in human RTT patients without any side effects (Kaufmann et al., 2016).

Furthermore, another study on a mouse model has proven that the main cause of the disorder is thought to be insufficient levels of MeCP2, specifically in the central nervous system (CNS). In this study, while mice were generated with a normal level of Mecp2 in the nervous system, the Mecp2 in peripheral tissues was silenced. As result, all RTT-like phenotypes were absent, which once more shows, that the primary target in researching RTT should be the brain (Ross et al., 2016).

However, proper regulation of MeCP2 levels in the CNS is important because its overexpression in mice resulted in seizures and hypoactivity (Steinkellner et al., 2019). *Mecp2* duplication is known to be related to severe neurological phenotype showed the importance of a balanced amount of MeCP2 (Kaufmann et al., 2016).

In summary, these various mouse models give a better understanding of the pathogenesis of the RTT and show that the evolving research of this disorder may result in RTT becoming a curable condition in the future (Shah & Bird, 2017).

## 4.6. Hyperacetylation

Histone acetylation and deacetylation are associated with increased and decreased mRNA transcription respectively. A loss in the balance between these two processes often leads to abnormalities in gene expression, a common occurrence in various disorders. This is also the case in RTT. Here, MeCP2 mediates the deacetylation of core histone proteins which in turn results in the silencing of gene expression.
A number of MeCP2 mutations which are known to be implicated in RTT onset are associated with the loss of TRD function on the cellular level. Two such mutations are the missense R168X and V288X (803delG). The resulting MeCP2 truncation products lack the intact TRD. This in turn leads to the hyperacetylation of H3 at K16 (Wan et al., 2001).

TRD on itself has been shown to be necessary but not sufficient for proper deacetylation. The H3 of mice carrying a stop codon mutation immediately downstream of T308 (a truncation, which, however retains the intact MBD and TRD domains), also exhibited a 2 to 3-fold increased acetylation (Shahbazian & Zoghbi, 2001). This finding underlines the importance of MeCP2's C-terminal portion in this process, possibly in stabilizing MeCP2/Sin3A/HDAC contacts.

Finally, *Mecp2*-null mice did not exhibit a maturation-dependent reduction in acetylated H3K9 in their neurons compared to their wild-type controls (Thatcher & LaSalle, 2006). Coupled with decreased K9 methylation in the mutant cells, these observations clearly point to the importance of MeCP2-mediated deacetylation in neuronal maturation.
Taken together, histone H3 hyperacetylation in cases of MeCP2 mutation are observed frequently. In the first two manuscripts, however, H4 acetylation levels remained unchanged, a finding that was also confirmed elsewhere (Urdinguio et al., 2007).

## 4.7. Inheritance of Rett Syndrome

On one hand, the sporadic form of RTT, that is assumed to be a d*e novo* mutation, usually happens once and randomly on the male copy of the X chromosome and is then passed on to the descendant. Thus, the genetic change is novel and is found in the somatic cells of the parents. Healthy siblings of a RTT patient also do not possess MeCP2 mutations (Österreichische Rett-Syndrom Gesellschaft, www.rett-syndrom.at).

On the other hand, the disorder can also be inherited from a mother that is phenotypically normal and has a germline mutation in the MeCP2 gene. This is why RTT occurs almost exclusively seen in females, as it follows an X-linked dominant pattern (Mari et al., 2005)

## 4.8. Diagnosis & Therapeutic strategies

RTT diagnosis is confirmed by sequencing in which the *MECP2* mutation is identified (Webb & Latif, 2001). Mutations of the *MECP2* gene have been recognized in about 90% of classical RTT patients (Nectoux et al., 2010). Nevertheless, the diagnosis is still based on clinical presentation and patients need to meet the clinical criteria. Mutations in the *MECP2* gene by themselves are not sufficient to make a diagnosis of RTT since *MECP2* mutations alone are also observed in other disorders (What Is Rett Syndrome, www.rettsyndrome.org). Typical laboratory results indicative for RTT are EEG and EKG abnormalities, atypical brain glycolipids, changed levels of neurotransmitter, creatinine and growth factor, as well as alkalosis (Ehrhart et al., 2016).

Present time spell promising developments in RTT research as more and more insight is acquired regarding the biology of MeCP2 as well as more possible of interventions that improve or reverse symptoms in mouse models are developed (Katz et al., 2016). These studies in mouse models show that re-expression of the wild-type *Mecp2* allele on the silenced X chromosome might overcome a lack of MeCP2 protein and consequentially, such reactivation can reverse phenotypes in late stage adult animals (Yu et al., 2011).

Therefore, the way to find a cure is to seek small molecules that can reverse the consequences of MeCP2 deficiency whereas another is to remedy the genetic cause of RTT by using gene therapy, gene correction or protein replacement (Shah & Bird, 2017).

Generally, the therapeutic targets that exist can be split in three categories:

- Targeting neurotransmitter systems in the brain, mostly Glutamate, GABA, Monoamines and Acetylcholin;
- Drugs that support growth factors, cell metabolism and homeostasis mostly by modulating the brain derived neurotrophic factors;
- Lastly targeting MeCP2 at the level of the gene, RNA or protein (Leonard et al., 2016);

However, the complexity of neurotransmitter balances, such as those involving glutamate and GABA, encourage a cautious approach since drug treatments may lead to deterioration of symptoms or serious side effects (Kaufmann et al., 2016).

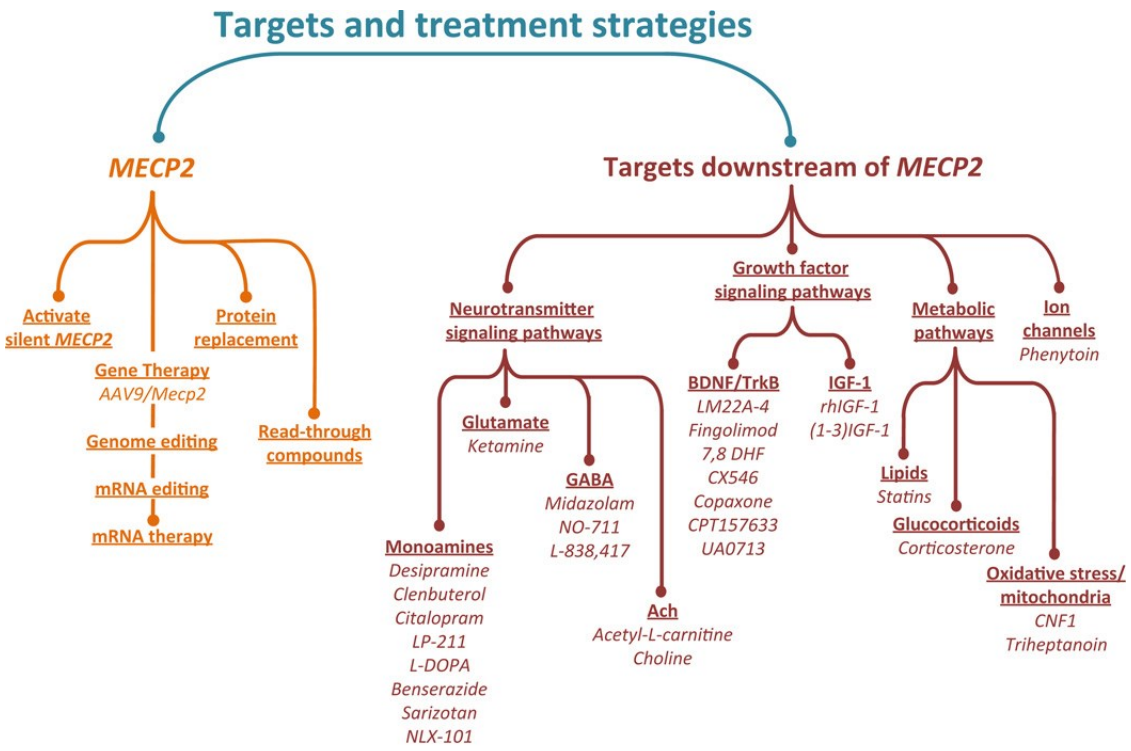


***Figure 2.*** *Targets and treatment strategies. Therapeutic targets and potential pharmacological strategies currently being explored in animal models for the treatment of Rett syndrome. Underlined headings indicate therapeutic target, while italics headings show compounds that have been reported in the literature to be effective.* (Reprinted by permission from Elsevier, Vol. number 39, Katz et al., 2016, Rett Syndrome: Crossing the Threshold to Clinical Translation).

Currently there is no cure for RTT, but there are physical therapies that can improve the quality of the patient's life and alleviate their symptoms.

Therapies include:

- Physiotherapy to maintain mobility and improve balance coordination
- Hydrotherapy for muscle relaxation and mobility stimulation in the water
- Occupational therapy to improve independence and fine motor functions
- Riding therapy to improve posture, balance and attention
- Speech therapy
- Music therapy to initiate targeted actions with hands on musical instruments (Österreichische Rett-Syndrom Gesellschaft, www.rett-syndrom.at).

All of the given therapeutic approaches face the challenges of tightly regulating MeCP2 protein levels in the CNS without leading to an overdose of MeCP2, which in turn can lead to severe neurological symptoms observed in patients affected with Xq28 duplication and mice

overexpressing MeCP2 (Katz et al., 2016) [Figure 2]. To quantify and allow the measurement of endogenous and exogenous MeCP2 protein levels in nuclear extracts from different cell lines and mice, an electrochemiluminescence-based Immunoassay was developed (ECLIA). This test was also used to show that a recombinant fusion protein, that contains the human MeCP2 isoform B protein and a minimal N-terminal HIV-TAT transduction domain (TAT-MeCP2), can raise the nuclear level of MeCP2 protein in neuronal cells after crossing the blood-brain barrier (Steinkellner et al., 2019).

In addition to therapeutic approaches, a number of general medications can help to relieve symptoms. These medications include:

- Selective serotonin reuptake inhibitors
- Beta-blockers for long-QT-syndrome
  (Chapleau et al., 2013)

Taken together, RTT is good for the development of targeted treatments due to the discovery of a common genetic cause, wide range of neurobiological data of postmortem and animals studies and a well – defined history of the disorder (Kaufmann et al., 2016).

## 4.9. Single-Cell isolation techniques

The generation and analysis of single cells has had a great impact on various fields of life science and biomedical research (Gross et al., 2015). Cell populations were considered homogenous and cell-based assays used the average responses of a population from thousand cells but without considering single cell phenotypes. However, studying single cells is needed to better understand the variation from cell to cell (Single Cell Isolation Trends: Technologies, Limitations & Applications, www.technologynetworks.com). It allows for monitoring phenotypic and genetic heterogeneity during cell growth, stress resistance and other biological processes as well as providing the possibility to select single cells with desired properties for biotechnology applications (Zhang et al., 2017).
Studies with mixed wild type and mixed mutants may not be as informative as single cells when it comes to cell to treatment response.

Cell isolation techniques can be split into two categories: the first deals with physical characteristics such as size, density, electric changes and deformability using methods

including density gradient centrifugation, membrane filtration, microchip-based capture platforms, laser microdissection and manual cell picking. The other is linked to cellular biological characteristics and protein expression properties and include affinity methods such as fluorescence-activated cell sorting (FACS) and magnetic-activated cell sorting (Hu et al., 2016).

Single cell isolation methods that were used in this thesis are Flow Cytometry (FC), QIAscout™ and limiting dilution cloning.

### 4.9.1. Cell sorting by Flow Cytometry (FC)

FC is one of the most frequently used technologies for single cell isolation. It uses laser excitation to characterize different cell types in a heterogenous cell population based on size, granularity and fluorescence. Cellular properties can be extracted with a forward scatter which indicates the size of the cell and side scatter which is indicative of the granularity and internal complexity of the cell (McKinnon, 2018). For the cell sorting a so-called FACS device is used. The special feature is the vibrational actuation in the apparatus, which breaks the liquid flow enriched with cell material into fine droplets. In this process, the liquid drops are chosen to be exactly large enough to have the size of just one cell (Gross et al., 2015). The device then applies a positive or negative charge to the droplet containing the cell of interest. An electrostatic deflection system helps to collect the charged droplets into collection tubes, slides or plates. FACS is normally used for isolation of highly purified cell populations but it is also able to isolate single cells of interest from thousands of cells (Hu et al., 2016).

### 4.9.2. QIAscout™

QIAscout (QIAGEN™) was developed for isolating single cells effectively and fast by 12.000 individual microrafts. Each microraft is 200 µm in length and 200 µm in width and serves as releasable culture site for individual cells or colonies. Seeding and cultivation of cells on the QIAscout™ array is comparable to standard cell culture vessels. QIAscout™ arrays are mounted on inverse microscopes to allow selection and picking of individual microrafts. A needle pierces through the lower surface of the array and dislodges the microraft of interest with its cell attached. The microraft can then betransported to a 96-well plate using a

magnetic wand. This method contains cell isolation and recovery with cells remaining viable (QIAscout User Manual, QIAGEN, www.qiagen.com).

### 4.9.3. Limiting Dilution Cloning

Limiting Dilution Cloning is a well-established method for the production of monoclonal cell cultures. It is based on a dilution of a suspension of cells in several dilution steps up to the last dilution in which statistically only one or no cell is present. The probability to achieve a specific number of cells per aliquot is defined by Poisson's distribution.
The final dilutions depending on the cell number in the starting population are then placed in wells and incubated for further cultivating (Gross et al., 2015).

The aims of this work are to establish an appropriate cell model in order to advance the development of therapies for RTT. For this purpose, the three aforementioned methods are used to isolate single cells. Clones will be then characterized by immunofluorescence staining, the HUMARA assay and Sanger sequencing. All experiments are carried out in human dermal fibroblasts (HDF) derived from female RTT patients with two different mutations, 705delG and T158M.

# 5. Aims of the thesis

The aim of this work was to establish an appropriate cell model in order to advance the development of therapies for RTT. For this purpose, three methods, Flow cytometry (FC), limiting dilution cloning and QIAscout™, were used to isolate single cells and obtain monoclonal cells such as mutant and wildtype MeCP2 clones. Numerous seedings were performed; clones were treated with various mediums, cells were immortalized and transfected with the plasmid pCl neo-hEST2 via electroporation. Clones were then characterized by immunofluorescence staining, the HUMARA assay and Sanger sequencing.

Furthermore, the status of histone hyperacetylation in monoclonal cells, which is essential in RTT, was determined by western blot with an antibody directed against acetylated histone H3 at Lys9 (H3k9).

All experiments were carried out in human dermal fibroblasts (HDF) derived from female RTT patients with two different mutations, 705delG and T158M.

# 6. Materials and Methods

## 6.1. Reagents

***Table 2.*** *Reagents that were used for all experiments*

| **Product** | **Product number** | **Company** |
|---|---|---|
| 0,05% Trypsin-EDTA | 25300-054 | Gibco |
| 2-Mercaptoethanol | M3148 | Sigma-Aldrich |
| 3% NGS – Normal Goat Serum Blocking Solution | S-1000 | Vector |
| Alexa Fluor 488 Goat Anti-Mouse | A11029 | Invitrogen |
| Alexa Fluor 488 Goat Anti-Rabbit | A11034 | Life technologies |
| Alexa Fluor 568 Goat Anti-Mouse | A11031 | Life technologies |
| Amniopan, Complete Medium for Amniotic Fluid Cells and CVS | #P04-70500 | PAN-Biotech |
| Anti-acetyl-Histone H3 (Ac-Lys$^{9}$) antibody produced in rabbit, 1:2500 | H9286 | Sigma-Aldrich |
| ATRX (D-5) SC-55584 mouse monoclonal IgG | CO217 | Santa Cruz Biotechnology |
| Biozym LE Agarose | 840004 | Biozym |
| Bovine Serum Albumin (heat shock fraction, pH 7, ≥98%) | A9647 | Sigma-Aldrich |
| ChemiGlow West Chemiluminescence Substrate Kit | 60-12596-00 | ProteinSimple |
| Cutsmart Buffer (10x concentrate) | B7204S | BioLabs |
| Di-Sodium hydrogen phosphate dihydrate | 106580 | Merck |
| DMSO | D2650 | Sigma-Aldrich |
| DNeasy ® Blood & Tissue Kit | 69506 | Qiagen |
| Dream Taq Master Mix | K1081 | Thermo Scientific |
| Dulbecco's Modified Eagle's Medium (DMEM) | 41966-029 | Gibco |
| Dulbecco's Phosphate Buffered Saline | D8537 | Sigma-Aldrich |
| Embedding medium; Prolong$^{tm}$ diamond Antifade Mountant with DAPI | P36966 | Invitrogen |
| Enzyme Hpa II | R0171 | BioLabs |
| Ethanol | 100983 | Merck |
| FBS Fetal Bovine Serum | F9665 | Sigma-Aldrich |
| G418 Disulfate salt solution | G8168 | Sigma-Aldrich |
| Gel Loading Dye Purple (6x) | B7024S | BioLabs |
| GeneRuler 1 kb Plus DNA Ladder | SM1333 | Thermo Scientific™ |
| Glycerol | G2025 | Sigma-Aldrich |

| | | |
|---|---|---|
| Glycine | 50046 | Sigma-Aldrich |
| Goat Anti Rabbit Antibody | A11011 | Invitrogen |
| HEPES | H3375 | Sigma-Aldrich |
| HotStarTaq Master Mix | 157042352 | Qiagen |
| Hydrochloric acid | 258148 | EMD Millipore |
| IGEPAL® | CA-630 | Sigma-Aldrich |
| iScript Reverse Transcription Supermix | 6416427 | Bio-Rad |
| iScript$^{tm}$ gDNA Clear cDNA Synthesis Kit | 172-5035 | Bio-Rad |
| Karyomax Colcemid | 15210040 | Gibco |
| Magnesium chloride hexahydrate | M2393 | Sigma-Aldrich |
| Marker: GeneRuler 1kb Plus DNA ladder | SM1333 | Thermo Scientific |
| MassRuler DNA Loading Dye (6X) | R0621 | Thermo Scientific™ |
| MECP2 1:100/1:400 | WH0004204M1 | Sigma-Aldrich |
| MECP2 XP | 3456 | Cell Signaling Technology |
| MECP2_RT_Ex3_F, 5'-AGCTTAAGCAAAGGAAATCTGGCC-3' | | Eurofins MWG Operon |
| MECP2_RT_Ex4_R, 5'-GGAAGCTCCTTGTCAAGATGCCT-3' | | Eurofins MWG Operon |
| Methanol | 106009 | Merck |
| Midori Green Advance | 617004 | Biozym |
| Monoclonal Anti-β-Tubulin antibody produced in mouse, 1:1500 | T4026 | Sigma-Aldrich |
| N,N,N',N'-Tetramethylethylendiamin (TEMED) | 110732 | Merck |
| Na2EDTA | E-5134 | Sigma-Aldrich |
| PenStrep | 15140-122 | Gibco |
| Pierce$^{tm}$ 16% formaldehyde (w/v), Methanol-free | 28906 | Thermo Scientific |
| Pierce™ BCA Protein Assay Kit | 23227 | Thermo Scientific™ |
| Potassium chloride | 104936 | Merck |
| Potassium dihydrogen phosphate | 104873 | Merck |
| ProSieve™ 50 Gel Solution | 50618 | Lonza |
| Red HS Taq Master Mix | 331126 | Biozym |
| RNeasy Plus Mini Kit | 74134 | Qiagen |
| Sodium chloride | S3014 | Sigma-Aldrich |
| SURE/Cut Buffer L for Restriction Enzymes (10x concentrated) | 13674400 | Roche |
| TAKARA LA Taq | RR02AG | Takara |
| Tricine | T0377 | Sigma-Aldrich |
| Triton™ X-100 | T8787 | Sigma-Aldrich |

| | | |
|---|---|---|
| Trizma® base (= TRIS) | T6066 | Sigma-Aldrich |
| Trypan Blue | 111732 | Merck |
| TWEEN® 20 | P9416 | Sigma-Aldrich |

## 6.2. Solutions and buffers

TBE buffer (10x), pH= 8.3

***Table 3***. *Components of the TBE buffer*

| **Substance** | **Weighed portion** |
|---|---|
| TRIS base | 108 g |
| Boric acid | 55 g |
| $Na_2EDTA$ | 9.3. g |
| $ddH_2O$ | Ad 1 l |

The buffer was autoclaved and stored at room temperature.

PBS (10x), pH = 7.4

***Table 4.*** *Components of PBS (10x), pH= 7.4*

| **End concentration (1x PBS)** | **Substance** | **Weighed portion (10x PBS)** |
|---|---|---|
| 137 mM | NaCl | 80 g |
| 2.7 mM | KCl | 2 g |
| 5.4 mM | $Na_2HPO_4 \cdot 2\ H_2O$ | 9.6 g |
| 1.5 mM | $KH_2PO_4$ | 2 g |
| | $ddH_2O$ | Ad 1 l |

The solution was autoclaved and stored at RT.

Tris-HCl (1M, pH = 6.8)

***Table 5.*** *Components of Tris-HCl*

| **Substance** | **Weighed portion** |
|---|---|
| TRIS | 121.14 g |
| $ddH_2O$ | ad 1000 ml |

Initially, 800 ml $ddH_2O$ were added, then the pH was adjusted and finally the remaining water was supplemented.

PBST (PBS + 0.05% Tween 20)

***Table 6.*** *Components of PBST*

| **Substance** | **Weighed portion** |
|---|---|
| 10x PBS | 100 ml |
| TWEEN® 20 | 0,5 ml |
| $ddH_2O$ | Ad 1000ml |

The solution was stored at 4°C.

Electrophoresis Buffer

***Table 7.*** *Components of the Electrophoresis Buffer*

| **Substance** | **Weighed portion** |
|---|---|
| TRIS/Tricine (10x) | 100 ml |
| 10% SDS solution | 10 ml |
| $ddH_2O$ | Ad 1 l |

The solution was stored at 4°C.

Tris-Tricine (10x) Buffer

***Table 8.*** *Components of the Tris-Tricine Buffer*

| **Substance** | **Weighed portion** |
|---|---|
| TRIS | 121 g |
| Tricine | 179 g |
| $ddH_2O$ | Ad 1 l |

The solution was autoclaved and stored at 4°C.

Blotting Buffer

***Table 9.*** *Components of the Blotting Buffer*

| **Substance** | **Weighed portion** |
|---|---|
| TRIS-Glycine (10x) | 100 ml |
| Methanol | 200 ml |
| 10% SDS solution | 200 µl |
| $ddH_2O$ | Ad 1 l |

The solution was stored at 4°C.

Tris-Glycine (10x) Buffer

***Table 10.*** *Components of the Tris-Glycine Buffer*

| **Substance** | **Weighed portion** |
|---|---|
| TRIS | 30 g |
| Glycine | 144 g |
| $ddH_2O$ | Ad 1 l |

The solution was autoclaved and stored at 4°C.

## 6.3. Materials

***Table 11.*** *Materials that were used for all experiments*

| **Product** | **Product number** | **Company** |
|---|---|---|
| 96/24/6 Well plates | 655161 | Greiner Bio-One |
| B.Braun Omnifix®–F Tuberculin syringe with Luer connection | 9161406V | Braun |
| Cellstar® cell culture flasks 25cm$^2$/75 cm$^2$/175 cm$^2$ | 690160/658170/660160 | Greiner Bio-One |
| Centrifuge tubes 15ml /50ml | 352096/ 352070 | Falcon® |
| Counting slides, dual chambers for cell counter | 145-0011 | Bio-Rad |
| Cryotubes | 479-1220 | VWR |
| Eppendorf® micropestle (for 1.2 - 2 mL tubes) | Z317314 | Sigma-Aldrich |
| Eppendorf® Safe-Lock microcentrifuge tubes volume 1.5 mL, natural | EP0030120086 | Sigma-Aldrich |
| Falcon® Round-Bottom Tubes with Cell Strainer Cap, 5 mL | 38030 | Stemcell Technologies |
| Glass Beads (acid-washed, 425-600 µm) | G8772 | Sigma-Aldrich |
| Microscope Cover Glass 24x60mm # 1,5 Menzel-Gläser | 4657519 | Thermo Scientific™ |
| Microscope Slides - SuperFrost®Plus 25x75x1.0mm | J1800AMNZ | Thermo Scientific™ |

| | | |
|---|---|---|
| Microplate (96 Well, PS, F-BOTTOM, clear, sterile) | 655161 | Greiner Bio-One |
| Nadel 0,9 mm diameter, Sterican Gr.1, G 20x1 ½ ø 0,90 x 40 mm, yellow | 4657519 | Braun |
| Pierce™ Tissue Strainers (250 µm, 2.5 mL) | 87791 | Thermo Scientific™ |
| QIAscout 12000-Microraft Arrays | 928031 | Qiagen |
| QPCR qPCR Tube Strips 0.2 ml with single flat caps | 82-1502-A | PeqLab |
| Round cover glasses 12 mm No. 1 | 631-1577P | VWR |
| Sterile syringe filter w/0.2µm Cellulose | 514-0061 | VWR |

## 6.4. Technical equipment

- Agarose gel electrophoresis system, Mupid-One
- BD FACSAria ™Fusion Cellsorter, Biosciences
- $CO_2$ Incubator, #CB210, Binder
- Heraeus Multifuge X3FR Centrifuge, #75004536, Thermo Fisher Scientific
- Imager: FluorChem HD2, ProteinSimple
- Leica DMRB RB Mikroskop Microscope Fluorescence Fluoreszenz Auflicht Durchlicht DM RB Type 301-371.010
- Microcentrifuge 5415 R, Eppendorf
- NanoDrop™ 1000 Spectrophotometer, Thermo Fisher Scientific
- TC20™ Automated Cell Counter, #1450102, Bio-Rad
- Thermocycler Gene Amp® PCR System 9700 PE, Applied Biosystems
- Thermomixer comfort, Eppendorf

## 6.5. Cell lines

All experiments were carried out in human dermal fibroblasts (HDF) derived from female RTT patients (#GM07982 and #GM17880) obtained from the Coriell Cell Repositories (Coriell Institute for Medical Research, NJ, USA). Both cell lines were at passage 6 (P6) at the beginning of experiments.

***Table 12.*** *Overview of cell lines that were used for experiments showing various characteristics and phenotypic data* (Coriell Institute, https://www.coriell.org, GM17880B, GM07982A)*;*

| | **GM07982** | **GM17880** |
|---|---|---|
| **Cell Type** | Dermal fibroblast | Dermal fibroblast |
| **Sex** | Female | Female |
| **Age** | 25 years (At sampling) | 5 years (At sampling) |
| **Race** | White | White |
| **Gene** | MeCP2 | MeCP2 |
| **Chromosomal Location** | Xq28 | Xq28 |
| **Identified Mutation** | 705delG (frameshift mutation in the gene encoding methyl-CpG binding protein 2;) | Thr158Met (C>T transition at nucleotide 473 in exon 3 of the gene encoding methyl-CpG binding protein 2 resulting in the substitution of threonine 158 by methionin in the methyl-binding domain;) |
| **Phenotypic Data** | Microcephaly; Hand wringing that began at age 2 and became more intense; Atrophy; Scoliosis diagnosed at age 12; Severe Kyphoscoliosis at age 25; Early milestones were slow; Started losing skills at age 2; Currently severely retarded; No sleep problems; no self-injurious behavior; Abnormal EEG; | Growth and developmental delay; can walk only with assistance; nonverbal; no hand use; constant repetitive hand motions; Teeth grinding; Some sleep difficulties; Eating problems with minor reflux; Breath holding and Hyperventilation; Small feet; Some Tremor; No seizures but abnormal EEG; |

### 6.5.1. Morphology of cell lines

The following photographs [Figure 3] show HDF cells of two RTT patients that were used in all experiments. Both cell lines, c705delG (GM07982A) and T158M (GM17880B), slightly differ in morphology.

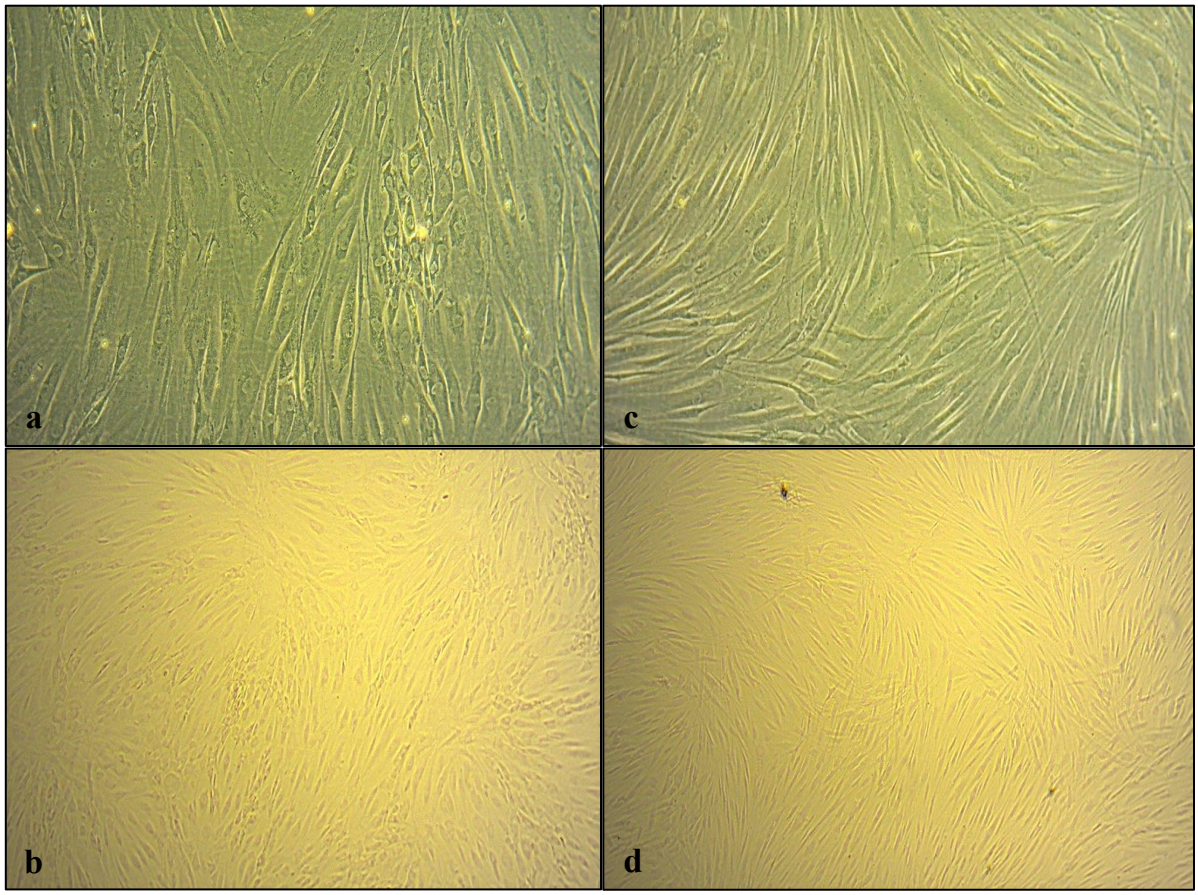


***Figure 3 a | b | c | d.*** *Microscope pictures of human Rett syndrome fibroblast cells at 40x magnification (a+c) and at 20x magnification (b+d).* ***a*** *|* ***b*** *GM07982A cells carrying the mutation c705delG look more oval.* ***c*** *|* ***d*** *GM17880B cells carrying the mutation T158M look more elongated.*

## 6.6. Cell culture

### 6.6.1. Thawing of cell lines

Cells were thawed quickly in a pre-warmed bead bath and transferred into a Falcon tube containing 8 ml culture medium (DMEM + 10% FBS + 1% PenStrep). Then, the cells were centrifuged for five minutes at 300 x g at room temperature. After removing the supernatant, the cells were re-suspended in 1 ml culture medium and transferred to a T25 flask (25cm$^2$)

containing 4ml fresh culture medium. The cells were grown in a humidified incubator at 37°C, 5% $CO_2$.

### 6.6.2. Cell splitting

Cells were split every two to three days after reaching 80-90% confluency and were passaged at a ratio between 1:2 to 1:4. First, the laminar air flow was wiped with 70% ethanol, then culture medium and trypsin-EDTA (0.05%) were pre-warmed in a bead bath to 37°C. After aspirating the medium from the cells, they were rinsed with DPBS. 0.05% trypsin-EDTA was added to the flask and incubated for five minutes at 37°C. Detachment of the cells was examined under the microscope. Then the cells were re-suspended in fresh culture medium by pipetting up and down and transferred to a new flask. Finally, the cells were mixed well by gently agitation and then incubated at 37°C, 5% $CO_2$.

For identification of contaminations with mycoplasma, cells were checked regularly by mycoplasma testing service (Eurofins Genomics).

### 6.6.3. Changing of Cell Culture Medium

A change of cell culture medium was necessary after 2 to 3 days after splitting. To achieve this, the medium was removed from the flask and replaced with fresh cell culture medium (DMEM + 10% FBS + 1% Penstrep).

### 6.6.4. Preparation of Conditioned Medium

Medium was aspirated from cultivated flasks and stored. After 10% FBS were added, the medium was filtered with a sterile syringe filter. The conditioned medium was stored at -20°C until use.

### 6.6.5. Cell freezing

Medium from a T75 flask (75$cm^2$) was aspirated from the cell layer and rinsed with 5 ml of DPBS. 2 ml trypsin-EDTA were added and incubated for five minutes at 37°C. After that, 9 ml of culture medium were added to the flask. Cells were passaged at a ratio of 1:3.

The rest of the cell suspension was transferred to a Falcon centrifuge tube and the cell number was determined. The Falcon tube was then centrifuged for five minutes at 300 x g and 20°C. After the supernatant was removed, the cell pellet was washed with 10 ml DPBS. The Falcon was then further centrifuged for another five minutes at 300 x g and 20°C. The cell pellet was re-suspended in freshly prepared freezing medium (DMEM + 20% FBS + 10% DMSO) at a concentration of 5 x 10^5 cells per cryo vial. Frozen cells were stored overnight at -80°C using a freezing container and then in the nitrogen tank.

#### 6.6.6. Karyotyping

1.5 x $10^5$ cells were seeded in a 6-well plate and grown overnight at 37°C in a humidified incubator with 5% $CO_2$. The next day, 50 µl colcemid solution (10g/ml, Karyomax) were added to each well and incubated for 30 minutes at 37°C. Then, the medium was removed from the cell layer and washed with DPBS.
Samples were treated for five minutes with 250 µl of trypsin-EDTA (0.05%) at 37°C, 5% $CO_2$. Afterwards, 1 ml of culture medium was added and cells were collected in a 50 ml falcon tube. Karyotyping was performed by the Cytogenetics Laboratory at the Institute of Medical Genetics, Medical University of Vienna.

### 6.7. Single cell Isolation Methods

The isolation of single cells was performed by using three different methods:
1.) Cell sorting (Flow cytometry)
2.) Limiting Dilution Cloning
3.) QIAscout

Cell lines were cultivated as described in section 6.6.. Cells were grown to 80-90% confluency.

#### 6.7.1. Cell sorting (FC)

FC was performed by the core facility at the Medical University of Vienna, AKH.
Both cell lines, carrying the 705delG and T158M mutation were split at a ratio of 1:4 at P9.

Then the cells of both strains were collected in separate tubes with a cell strainer snap cap (5ml round bottom tubes with 35 µm nylon mesh) and sorted by the BD FACSAria$^{tm}$ Fusion Cellsorter (BD Biosciences) into a 96-well plate containing 100 µl culture medium (DMEM + 10% FBS + 1% PenStrep).
Subsequently, 100 µl of conditioned medium were added to each well and incubated at 37°C, 5% $CO_2$. After seven days, all wells were examined under the microscope for single cells. Cells reaching 80-90% confluency were passaged into 24-well plates.

### 6.7.2. Limiting Dilution Cloning

For Limiting Dilution Cloning cells were split as described in the method section 6.6. with cells counted in a TC20 cell counter. This procedure involved 20 µl from the cell suspension were mixed together with 20 µl trypan blue solution in a microcentrifuge tube. 10 µl of cell-trypan blue suspension were transferred to a disposable hemocytometer. The number of live cells was counted using the automated cell counter.
Cell suspension was diluted to 1x $10^4$ cells/ml in fresh cell culture medium as follows:

10 cells/ml
20 cells/ml
50 cells/ml

The appropriate volume of cell suspension and conditioned medium was aliquoted into a sterile centrifuge tube. 100µl of conditioned medium were dispensed per well of 96-well plates using a multichannel pipette. The 96-well plates were transferred to a humidified incubator at 37°C, 5% $CO_2$ and were visually inspected under the microscope from seven to ten days to assess evidence of monoclonality. After reaching 80-90% confluency, cells were passaged into 24-well plates.

### 6.7.3. QIAscout™

The first step of this method was the preparation of a QIAscout™ array. It is important that the array does not dry out during handling. It was rinsed with 2 ml of DPBS twice for three minutes each. Then, the array was rinsed with 2 ml culture medium, for three minutes.

50 000 cells/2 ml were added to the QIAscout array and mixed gently. Then the array was transferred to a humidified incubator at 37°C, 5% $CO_2$ overnight.

The next day, we examined the array under the microscope to ensure cell attachment to the array and that a proper number of cells were available for cell picking.

The whole equipment for cell picking (all cables and power supply for controller, inverted microscope, magnetic wand, magnetic collection plate and controller) was wiped carefully with 70% ethanol and placed under the laminar air flow. 96-well plates were filled with 100 µl culture medium (DMEM + 20% FBS + 1% Penstrep). The QIAscout™ array was placed under the microscope and focused until the squares of the array were visible. The QIAscout™ array was removed and the button of the Qiascout™ controller was pushed until blinking and the needle (black dot) was focused. After that, the button of the controller was pressed again so the needle moved down. The QIAscout™ array was placed under the microscope again and the cells were picked separately. The picked cells were then collected with a magnetic wand and cells were transferred to a 96-well plate that was placed over a magnetic field.

After picking, another 100 µl of conditioned medium were added to each well. The 96-well plates were examined every two to three days and were passaged when reaching 80-90% confluency.

## 6.8. Genotyping

### 6.8.1. DNA Extraction

For DNA extraction, the DNeasy® Blood & Tissue Kit (#69506, Qiagen) was used. Cells were centrifuged (max. 5 x $10^6$ cells) for five minutes at 300 x g and resuspended in 200 µl DPBS. 20 µl proteinase K and 200 µl buffer AL were added to each tube. The mixture was then vortexed carefully and incubated in a thermomixer at 56°C for ten minutes. Then, 200 µl ethanol (96 %) were added and vortexed again.

The mixture was pipetted into a DNeasy Mini spin column placed in a 2 ml collection tube and centrifuged at 6.000 x g for one minute. The DNeasy Mini spin column was then placed in a new 2 ml collection tube. 500 µl buffer AW1 were added to the tube and centrifuged at 6.000 x g for one minute. After that, the DNeasy Mini spin column was placed in a new 2 ml

collection tube and 500 µl buffer AW2 were added and centrifuged at 16.000 x g for three minutes. The DNeasy Mini spin column was placed into a 1.5 ml microcentrifuge tube and the DNA was eluted with 100 µl buffer AE by pipetting directly onto the DNeasy membrane. Samples were placed on ice and the concentration was determined. Samples were stored at -80°C.

### 6.8.2. Human Androgen Receptor Assay (HUMARA Assay)

500 ng of isolated DNA were digested with 2 µl methylation-sensitive restriction enzyme Hpa II (#R0171, NEB) overnight at 37°C (total sample volume of 10 µl). To digestion mixture, 1 µl buffer (CutSmart Buffer, #B7204S, NEB) was also added.

On the next day, 1 µl of the restriction enzyme Hpa II was again added to the samples, followed by a 3h incubation at 37°C. For each sample, an undigested control without the restriction enzyme was incubated in the same fashion. Subsequently, the enzyme was inactivated by incubation at 65°C for 15 minutes. A polymerase chain reaction (PCR) was performed as follows:

The following primers were used:
Forward primer: PR2_F: TGACATAGCGAGAGCCCTGTG FAM
Reverse primer: RP2_R: TGGTGGGTTCTCTAGCTGGT

For the mastermix 4.5 µl $H_2O$, 6.25 µl HS MM Qiagen, 1 µl forward primer and 1 µl reverse primer per sample were added. 0.5µl of the digested DNA, as well as the undigested control were used for the PCR. The cycling parameters are shown in table 13.

***Table 13.*** *PCR cycling conditions*

| | | |
|---|---|---|
| Denaturation | 96°C | 3 min |
| Annealing | 96°C<br>60°C<br>72°C | 20 sec<br>20 sec<br>45 sec } 32x |
| Elongation | 72°C | 7 min |

To check whether the amplification was successful, the PCR products were visualized on a 2% Agarose gel.

### 6.8.3. RNA Extraction

For RNA extraction the RNeasy Plus Mini Kit, (#74134, Qiagen) was used. Approximately 1 x $10^7$ cells were collected by centrifuging at 300 x g at room temperature. Then the cells were disrupted by adding 350 µl buffer RLT Plus and 3.5 µl ß-Mercaptoethanol and were vortexed. The lysate was homogenized by passing through a 20-gauge needle (0,9 mm diameter) fitted to an RNase-free syringe five times.

The lysate was then transferred to a gDNA Eliminator spin column placed in a 2 ml collection tube. Samples were centrifuged for 30 seconds at 8000 x g. The column was discarded and 350 µl of 70% ethanol were added to the flow-through and mixed well by pipetting. Then 700 µl of sample were transferred to a RNeasy spin column placed in a 2 ml collection tube and centrifuged for 15 seconds at 8000 x g, 22°C. The flow-through was discarded. 700 µl buffer RW1 were added to the RNeasy spin column and centrifuged for 15 seconds at 8000 x g at 22°C. The flow-through was discarded again. 500 µl buffer RPE were added to the RNeasy spin column and centrifuged for 15 seconds at 8000 x g at 22°C. The flow-through was removed. 500 µl buffer RPE were added to the RNeasy spin column and centrifuged for two minutes at 8000 x g at 22°C to wash the spin column membrane. After, the RNeasy spin column was placed in a new 2 ml collection tube. Samples were centrifuged at 16.000 x g for one minute at 22°C.

Finally, the RNeasy spin column was placed in a new 1.5 ml collection tube. 30 µl RNase-free water was added directly onto the spin column membrane and centrifuged for one minute at 16.000 x g at 22°C to elute the RNA. The eluate was pipetted directly on the spin column membrane and centrifuged for one minute at 16000 x g at 22°C. Samples were placed on ice and the concentration was determined. Samples were stored at -80°C.

### 6.8.4. Reverse Transcription of RNA to cDNA

To remove any trace DNA from the sample, 0.5 µl iScript DNase and 1.5 µl iScript DNase Buffer were mixed by pipetting up and down for several times. 2 µl of the DNase master mix were added to a 14 µl RNA sample. RNase-free water was added for a total reaction volume of 16 µl. Samples were vortexed. The sample was placed in a thermal cycler with a heated lid on and used under the following conditions:

***Table 14.*** *PCR cycling conditions for transcription of RNA to cDNA*

| | | |
|---|---|---|
| DNA Digestion | 25°C | 5 min |
| DNase inactivation | 75°C | 5 min |
| Storage Conditions | 4°C; ice | until RT step |

cDNA Synthesis

4 µl iScript Reverse Transcription Supermix and 16 µl DNase-treated RNA template were mixed together by pipetting up and down several times. After that, the sample was placed in a thermal cycler with a heated lid on was used under following conditions:

***Table 15.*** *PCR cycling conditions for cDNA synthesis*

| | | |
|---|---|---|
| Priming | 25°C | 5 min |
| Reverse transcription | 46°C | 20 min |
| RT inactivation | 95°C | 1 min |
| Hold | 4°C | ∞ |

All PCR samples were kept at -20°C until use.

### 6.8.5. Preparation of cDNA from clonal cells for further sequencing

For sequencing of the clonal cells, three different types of mastermixes were attempted. The following primers were used:

Forward Primer: MECP2_RT_Ex3_F

5'-AGCTTAAGCAAAGGAAATCTGGCC-3' (Eurofins MWG Operon)

Reverse Primer: MECP2_RT_Ex4_R

5'-GGAAGCTCCTTGTCAAGATGCCT-3' (Eurofins MWG Operon)

Working solution of primers: 2 µl primer (stock concentration: 100 pmol/µl) + 18 µl nuclease-free water (concentration: 10 pmol/µl);

The following three master mixes were used for each sample:

A) Dream Taq Master Mix, #K1081, Thermo Scientific

B) Red HS Taq Master Mix, #331126, Biozym

C) TAKARA LA Taq Master Mix, #RR02AG, Takara

***Table 16.*** *Table of reagents that were added to the Mastermix A and B*

| **Mastermix (A, B)** | |
|---|---|
| Nuclease-free water | 6 µl |
| Forward-Primer | 1 µl |
| Reverse-Primer | 1 µl |
| Mastermix | 10 µl |
| | |
| **Mastermix (A, B)** | 18 µl |
| + | 2 µl cDNA |

***Table 17.*** *Table of reagents that were added to the Mastermix C*

| **Mastermix (C)** | |
|---|---|
| Nuclease-free water | 4,3 µl |
| GC-1 Buffer | 12,5 µl |
| dNTPs | 4,0 µl |
| Takara TAQ-Polymerase | 0,2 µl |
| Forward-Primer | 1 µl |
| Reverse Primer | 1 µl |
| | |
| **Mastermix (C)** | 23 µl |
| + | 2 µl cDNA |

Following PCR cycling conditions were applied:

***Table 18.*** *PCR cycling conditions for cDNA of clones*

| | | |
|---|---|---|
| Denaturation | 95°C | 3 min |
| Annealing | 95°C<br>61°C<br>72°C | 20 sec<br>20 sec<br>45 sec } 35x |
| Elongation | 72°C<br>4°C | 5 min<br>∞ |

All PCR products were then loaded onto 2% agarose gel. Afterwards, PCR products were passed on to a colleague for sequencing.

#### *6.8.5.1. 2% Agarose Gel Electrophoresis*

2 g of agarose were added to 100 ml TBE buffer (1x, pH= 8.3). The mixture had been boiled in the microwave until agarose was dissolved. A magnetic stirrer was placed into the glass and the solution was mixed. Then 10 µl Midori Green was added, mixed and poured into a gel tray with a comb. The gel was left for approximately 30 minutes to solidify.
5 µl Marker (Thermo Scientific, #SM1333) and 5 µl of PCR product were loaded onto agarose gel. To the samples, 1 µl of gel loading dye (6x, BioLabs, #B7024S) was added for TAKARA LA Taq Mastermix. Then the gel was run for 20 minutes at 135V and finally DNA was visualized under UV-light.

## 6.9. Immunofluorescence (IF)

For IF 24-well plates with round glass slides (12 mm) were used. On the bottom of each single well 0.5 ml growth media was added. Then, 200 µl of cell suspension (150.000 cells) were seeded onto the glass slide. The glass slide was pressed to the bottom with a pipette to avoid cell growth under the glass slide. The cells were incubated at 37°C, 5% $CO_2$ for 24 hours.

The next day the growth medium was aspirated from the plates and washed twice with DPBS. Then the cells were fixed with 4% formaldehyde in DPBS for 20 minutes at 4°C. The slides were washed twice with DPBS to completely remove formaldehyde. Permeabilization was performed with 0.1% Triton X-100 for five minutes at room temperature twice. Then the cells were blocked with 3% BSA in DPBS for 30 minutes at room temperature. Next, all samples were incubated with a primary antibody diluted in 3% normal goat serum (NGS, #S-1000, Vector) in DPBS over night at 4°C.

***Table 19.*** *Primary antibodies that were used for immunofluorescence staining*

| **Primary antibody** | **Dilution IF** | **Product Number** | **Company** |
|---|---|---|---|
| MECP2 XP | 1:200 | 3456 | Cell Signaling Technology |
| ATRX mouse monoclonal IgG | 1:100 | CO217 | Santa Cruz Biotechnology |

After washing all samples twice with DPBS for five minutes, the samples were incubated with the appropriate secondary antibody in 3% NGS in DPBS at room temperature for one hour protected from light.

***Table 20.*** *Secondary antibodies that were used for immunofluorescence staining*

| Secondary antibody | Dilution IF | Product Number | Company |
|---|---|---|---|
| Alexa Fluor 568 goat anti mouse | 1:250 | A11031 | Life technologies |
| Alexa Fluor 488 goat anti rabbit | 1:250 | A11034 | Life technologies |

Then the samples were washed with DPBS for five minutes for three times. An embedding medium containing DAPI was pipetted onto the slides carefully avoiding air bubbles. Finally, the samples were stored at room temperature for drying. After 24 hours, the objects were examined under the confocal microscope.

## 6.10. NEON Transfection

For further experiments and single cell isolation, both cell lines were immortalized by transfection with the plasmid pCl neo-hEST2 (#1781, Addgene) via electroporation using the NEON transfection system (Invitrogen).

Cells were trypsinized, collected in a 50 ml Falcon tube and the cell number was determined. The cells were centrifuged for five minutes at 300 x g, 20°C and the pellet was washed with DPBS. Then, the pellet was re-suspended in NEON resuspension buffer at 1 x $10^7$ cells/ml and 5 µg of the plasmid was added. After incubation for five minutes at room temperature, cells were electroporated using the following parameters: 1000 mV, 60 ms, 1 pulse. Electroporated cells were added to an Eppendorf tube with 900 µl culture medium. Finally, the cell suspension was seeded in a 6-well-plate with 1 ml culture medium. Three days after transfection, the selection with 150 µg/ml G418 was started.

Cells were treated with 2 µg G418/ml disulfate salt solution during cultivation. Cell culture process remained as described in the method section 6.6.. For single cell isolation the QIAscout method was used.

## 6.11. Western Blot

### 6.11.1. Sample Preparation

The protein solutions were diluted with double-distilled water achieving an end concentration of 100 µg per sample. 4X Laemmli protein sample buffer (#1610737, Bio-Rad) and 10% 2-Mercaptoethanol had been added and then the samples were incubated at 95°C for five minutes.

### 6.11.2. Gel Electrophoresis

The gel was placed in the electrophoresis unit and Electrophoresis Buffer was poured until the gel was completely covered. The combs were removed and 24 µl or 40 µl of the samples as well as 5 µl of the marker (#26616, Thermo Fisher) were loaded in the wells of the polymerized gel. The gel ran with 100 V at 4°C for 90 minutes.

### 6.11.3. Transfer

The stacking gel was removed and a sandwich containing the separating gel and a membrane was built. This sandwich consisted of the Blotting Buffer wetted sponge, a wetted blot paper, the gel, a wetted membrane, another wetted blot paper and sponge. After building the sandwich, air bubbles were removed. Then, the sandwich was placed in the electrophoresis unit which had to be filled with Blotting Buffer. The transfer was performed with 0.3A for one hour. Afterwards, the transfer was checked by staining the membrane with Ponceau S. The membrane was cut into three parts and washed with PBS for decoloring.

### 6.11.4. Blocking

The membranes were blocked with 5% milk powder in PBST (PBS + 0.05% Tween 20) for at least one hour at room temperature.

### 6.11.5. Antibody Incubation

***Table 21.*** *Antibodies that were used for the antibody incubation*

| **Antibody** | **Dilution Western Blot** | **Product Number** | **Company** |
|---|---|---|---|
| Anti MeCP XP(D4F3) XP® Rabbit mAb | 1:1000 | 3456 | Cell Signaling Technologies CST |
| Monoclonal Anti-β-Tubulin antibody produced in mouse | 1:1500 | T4026 | Sigma-Aldrich |
| Anti-acetyl-Histone H3 (Ac-Lys$^{9}$) antibody produced in rabbit | 1:2500 | H9286 | Sigma-Aldrich |

The primary antibodies were applied in different dilutions in 5% milk powder in PBST and incubated in 50 ml Falcon tubes with gentle shaking overnight at 4°C.

The next day, the membranes were washed with PBST three times for five minutes. Then the secondary antibodies, diluted in 5% milk powder, were applied for at least one hour at RT. After this incubation step the membranes were washed with PBST three times for five minutes again. Finally, the substrate (ChemiGlow) was applied for five minutes. Thus, immunoreactive bands were visualized by chemiluminescence and ChemiDoc Imaging System (Bio-Rad) was used for recording the images.

# 7. Results

## 7.1. Karyotyping

Karyotyping was performed on c705delG and T158M cell lines, in order to determine the number of chromosomes as well as to check whether abnormalities were present. For the karyotyping experiment male control cells, AG21708A, were treated with colcemid for varying periods of time (30 minutes, one, two, three and four hours). This was done to determine which incubation time would work best. The optimal incubation time was found to be 30 minutes and this incubation period was used for the karyotyping of both primary fibroblast cell lines with the mutation c705delG and T158M. The photographs of the chromosomes and evaluations were then done by colleagues of the Cytogenetics laboratory department, Medical University of Vienna, and were made available to us. Both photographs have confirmed that the cell lines are from two female patients with 46 chromosomes including a set of X chromosomes (46, XX) [Figure 4 a, b].

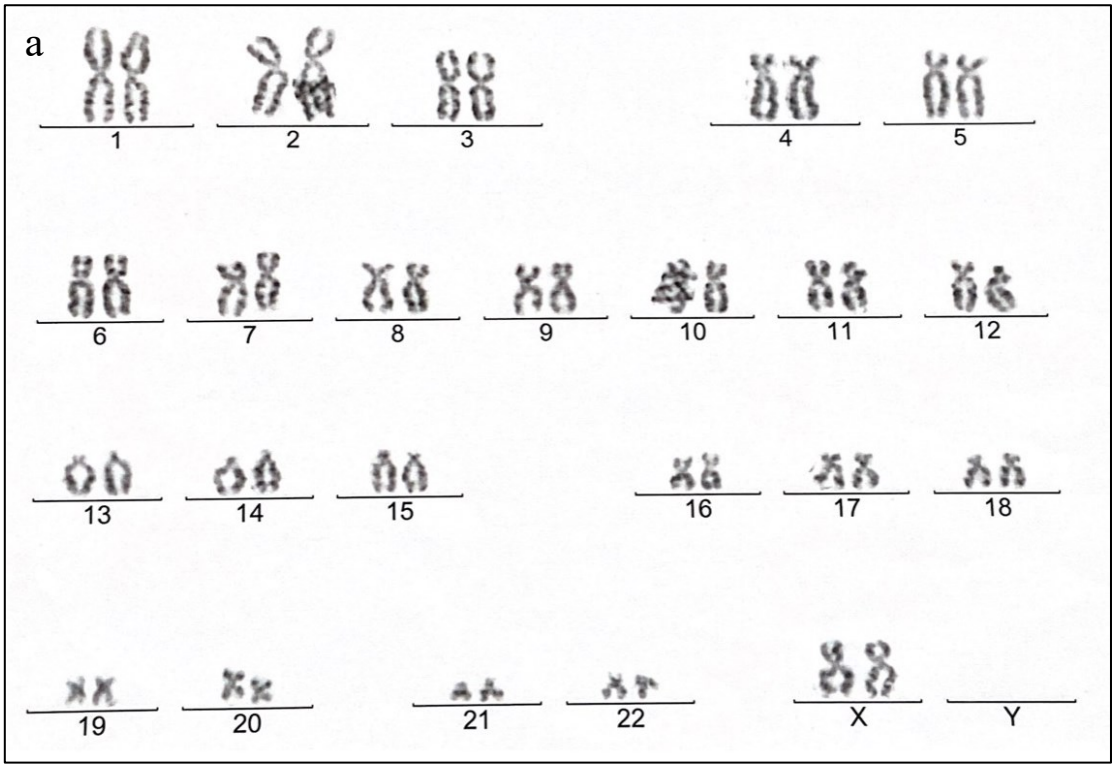

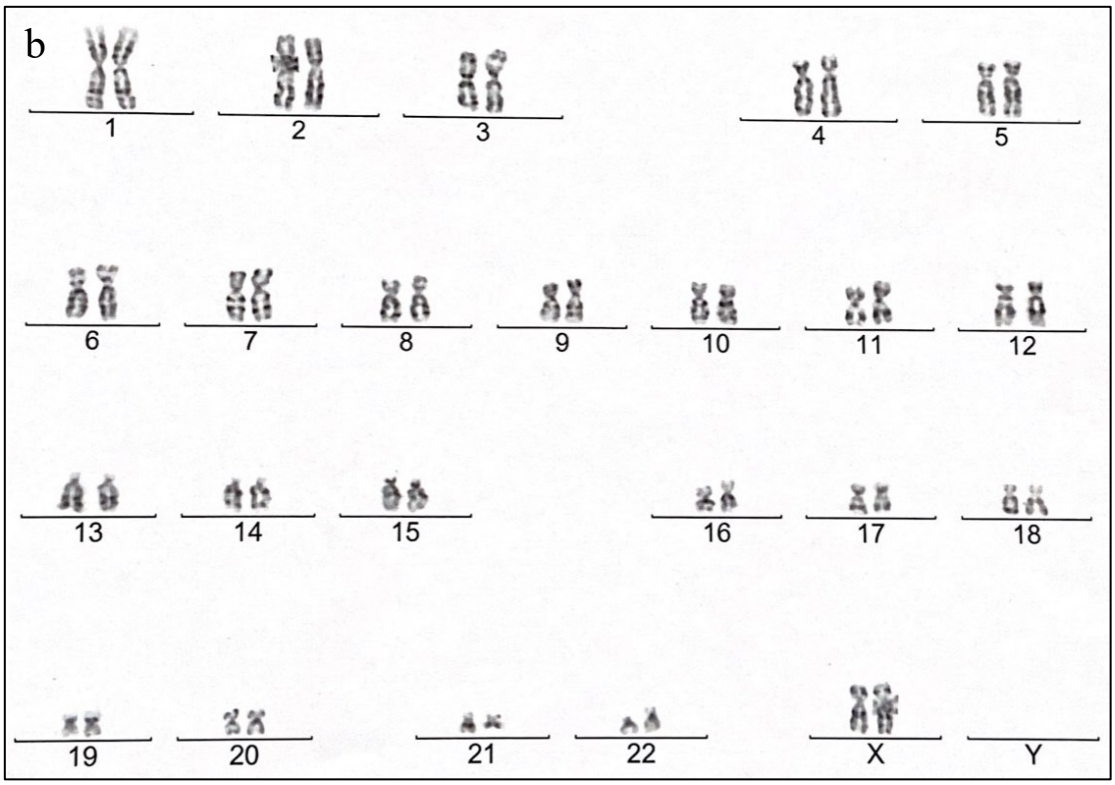


***Figure 4 a | b.*** *Results of Karyotyping confirmed that cell lines are from two female patients with 46 chromosomes including a set of X chromosomes (46, XX).* ***a*** *| Cell line GM07982A with the mutation c705delG.* ***b*** *| Cell line GM17880B with the mutation T158M.*

## 7.2. Comparison of methods for single cell seeding

The aim of the project is to preserve a single cell that will be used to create a cell culture model with the same properties of that original cell (Bernice M. Martin, 2008). Therefore, it is important to devise a proper and reliable method for single cell picking. Out of a broad range of methods, three different ones were selected; all have their advantages and drawbacks. The differences between those methods are presented here.

### 7.2.1. Limiting Dilution Cloning

Limiting dilution cloning is a series of dilutions, which depends on a calculation for a single cell per a given volume. It is a simple method that does not require any specialized equipment or advanced handling (Bernice M. Martin, 2008). In order to isolate individual cells in single wells, the cells are seeded at an average density of less than one cell per well, which means that wells with no cells as well as some wells with multiple cells may exist (Improving Clone Isolation and Screening In Hybridoma Cells, www.cellculturedish.com). Therefore, there is no 100% guarantee of isolating only single cells.

### 7.2.2. QIAscout™

QIAscout™ is a newer method to isolate single cells. Its advantage is that cells can be directly observed under microscope and the cells of interest can be manually targeted [Figure 5]. Due of its manual picking function, this technique is more time-consuming and labor-intensive. In addition, the equipment requires an inverted microscope.

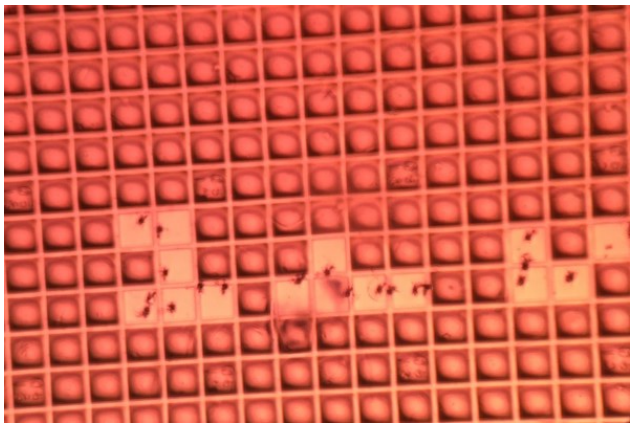

***Figure 5.*** *QIAscout™ array from the microscope's lens perspective after picking cells of interest (20x magnification).*

Single cell clones need to be cultivated for a long time after the single cell picking. It is very important to make sure that everything is sterile. To achieve this, needles as well as the magnetic wand have to be disinfected often. The results [Table 22] which showed that mostly positive MeCP2 and negative MeCP2 clones picked with QIAscout™ in comparison to the other single cell seeding methods make it a reliable method with the main drawbacks being sterility issues.

### 7.2.3. Cell sorting by Flow Cytometry (FC)

Finally, FACS is highly efficient in cell sorting because thousands of cells can be sorted in a very short period. This reduces the experimental costs and time that is normally used for single cell picking (Valihrach et al., 2018). The automated system is linked to computer software, which allows the user to program the criteria for the cell that would be selected. Then the equipment performs single cell isolation and plates the cells of interest without the need for manual pipetting. The automation makes this method easy and reliable. Moreover, more cells can be tested compared to other methods allowing single cell seeding to be

accomplished much faster (Improving Clone Isolation and Screening In Hybridoma Cells, www.cellculturedish.com).

Another feature of FC is that while the process is automated, contamination is very rare.

## 7.3. Seedings

The use of the three different methods of single cell isolation and various treatments with medium as well as immortalized cells, has given rise to the following results:

***Table 22.*** *Clonal cells overview showing results after various seedings with different mediums: CM: Conditioned Medium; Culture medium: DMEM + 10% or 20% FBS+ 1% Penstrep; G418: Disulfate Salt Solution; Amniopan; Methods: FC: Flow Cytometry, L.D.: Limiting Dilution;*

| | **MeCP2 positive clones** | **MeCP2 negative clones** | **Method** |
|---|---|---|---|
| **CM + culture medium** | 32 | 2 | FC, L.D., QIAscout™ |
| **CM + culture medium + G418** | 9 | 4 | L.D., QIAscout™ |
| **Culture medium + G418** | 4 | - | L.D. |
| **CM + culture medium + Amniopan** | - | - | L.D. |

Ten 96-well plates were seeded using the three methods – QIAscout™ [Figure 6], limiting dilution and FC. The medium was changed every two to three days. Single cells were further cultivated with *Conditioned Medium (+20% FBS) and fresh culture medium (DMEM +20% FBS + 1% PenStrep)*.

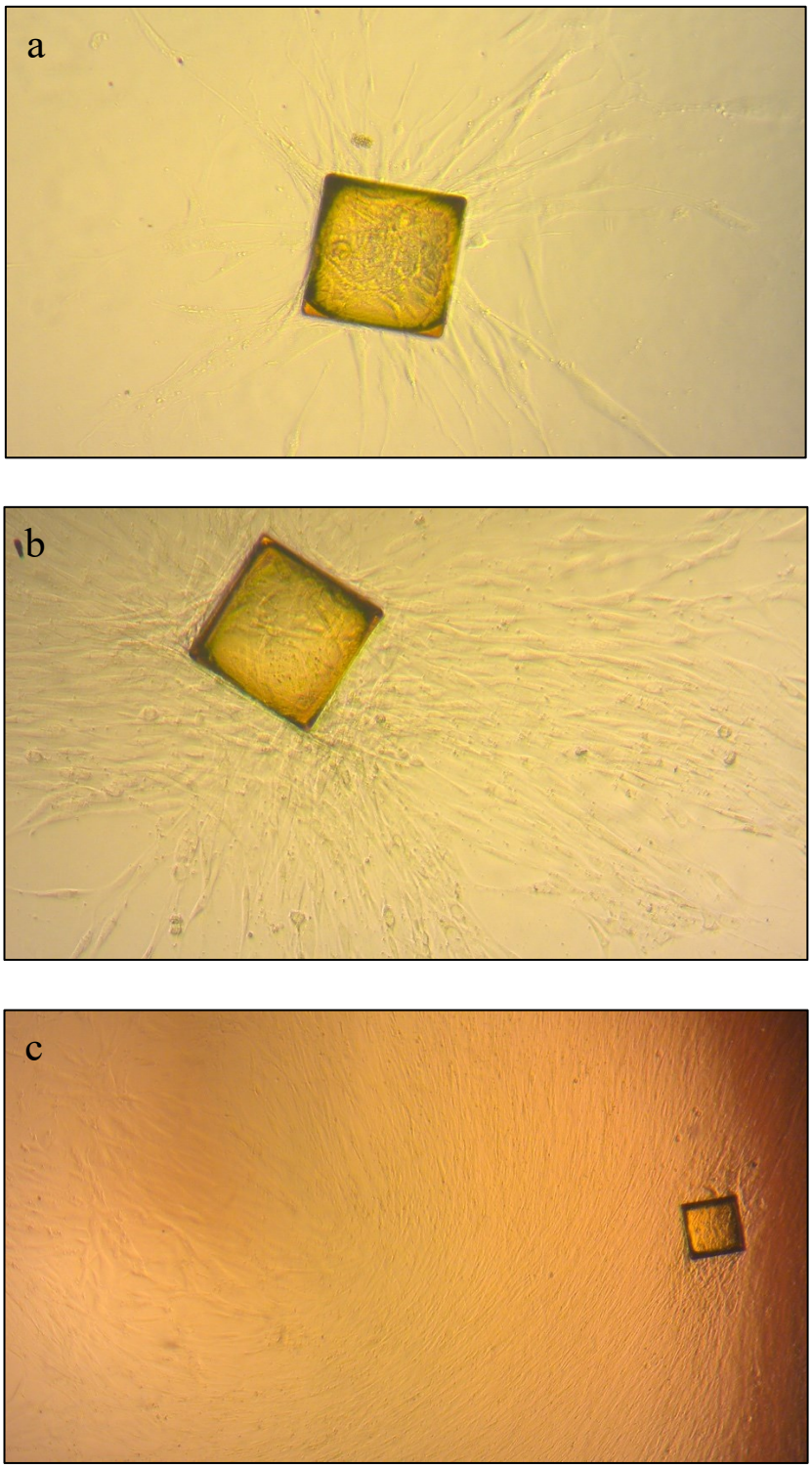


***Figure 6 a | b | c.*** *Development of QIAscout seeding.* ***a |*** *7 days after QIAscout picking at 20x magnification;* ***b |*** *14 days after QIAscout picking at 20x magnification;* ***c |*** *21 days after QIAscout picking at 10x magnification;*

Passage number of cell lines at time of first seeding:

FC T158M: Passage 9

c705delG: Passage 9

| | |
|---|---|
| Limiting Dilution | T158M: Passage 11 |
| | c705delG: Passage 9 |
| QIAscout™ | T158M: Passage 12 |
| | c705delG: Passage 11 |

***Table 23.*** *Number of 96- well plates that were used at first seeding*

| | **QIAscout** | **Limiting Dilution** | **FC** |
|---|---|---|---|
| **c705delG** | 1x 96-well | 2x 96-well | 2x 96-well |
| **T158M** | 1x 96-well | 2x 96-well | 2x 96-well |

After approximately one-month cultivation, clones were transferred from 96-well plates to 24-well plates. Clones were further cultivated with *culture medium*.
Four weeks after seeding, QIAscout™ plates became contaminated and were thrown away. FC plates were senescent after approximately five weeks since first seeding and stopped growing. Six weeks after first seeding, the limiting dilution 96-well plates were also thrown away because no more clones were confluent and therefore no more clones could be moved to 24-well plates.

**Results:** T158M

18 clones – all of them were wildtype MeCP2.

c705delG

four clones – one wildtype (MeCP2 positive), two mutants (MeCP2 negative), one mixed.

Clones that were obtained and isolated, were characterized by immunofluorescence staining, HUMARA Assay and sequencing.
FC seeding yielded two clones from the 96-well plates. However, cells from FC plates did not grow properly and became senescent soon. Since cells with the mutation c705delG gave promising results in the first seedings, only this cell line was verified in further.

In further seedings, cells were attempted to be immortalized and transfected with the plasmid pCl neo-hEST2 (#1781, Addgene) using the NEON transfection system (Invitrogen) and were selected with 300µg/2ml G418 (Disulfate salt solution, #G8168, Sigma) [Figure 7]. The medium was changed every two to three days. Clones were further cultivated with

*Conditioned Medium (+20% FBS) and fresh culture medium (DMEM +15% FBS + 1% PenStrep) + 2 µl G418/ml*.

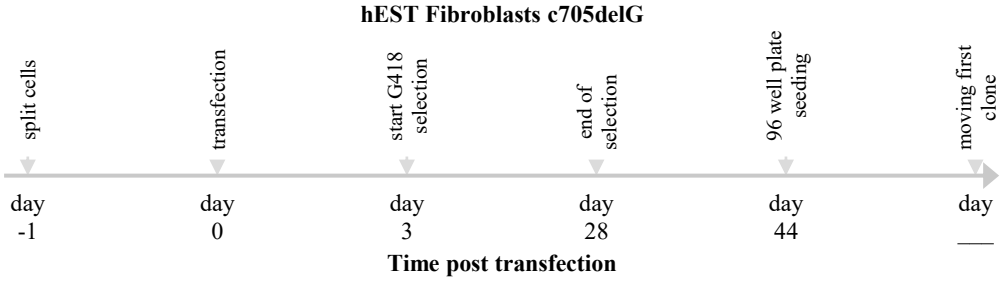


***Figure 7.*** *Timeline showing development of cell cloning from day one until moving first clone.*

***Table 24.*** *Number of 96- well plates that were used at another seeding*

| | **QIAscout** |
|---|---|
| **c705delG** | 1x 96-well |

Approximately four weeks after single cell picking, first clones were moved from 96-well to 24-well plates. Six weeks after picking cells, the 96-well plates became confluent.

**Results:** c705delG

five clones – all cells were wildtype MeCP2.

Additional seedings were performed using the limiting dilution method. Cells were cultivated with *culture medium + 2 µl G418/ml* or *conditioned medium + culture medium + Amniopan* or *conditioned medium + culture medium + 2 µl G418/ml*.

**Results:** c705delG

24 clones – 20 wildtype (MeCP2 positive), 4 mutants (MeCP2 negative).

To investigate whether the G418 treatment results in MeCP2 read-through and therefore positive immunofluorescence staining in MeCP2 mutant cells, non-transfected dermal fibroblast c705delG cells were treated with G418 together with a negative control. The results showed that abundance of wild type clones occurs independently of G418 treatment [Figure 8].

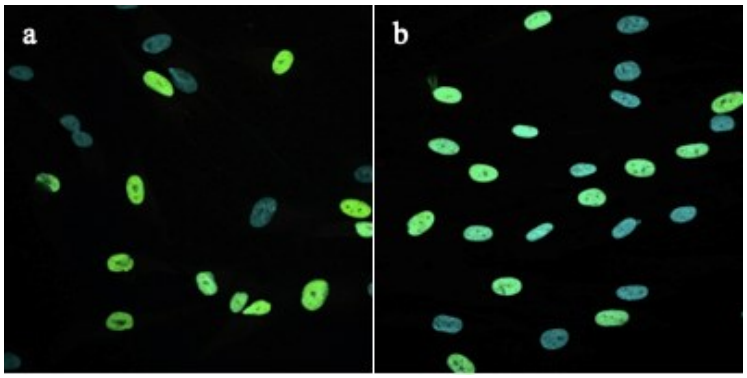


***Figure 8 a | b**. IF images (20x magnification) showing non transfected dermal fibroblast c705delG cells treated with and without G418. Cell counting showed that abundance of wild type clones occurs independently of G418 treatment. **a** | Cells treated with G418 (pos.: 12; neg.: 10; total 22 cells;) **b** | Cells without G418 treatment (pos.:16; neg.:9; total: 25cells;).*

## 7.4. Determination of the genotype of the c705delG cell line

### 7.4.1. Confirmation of monoclonal cells by HUMARA Assay

To confirm the genotype of MeCP2 cells of the cell line carrying the mutation c705delG, the DNA of each clone was isolated (DNeasy ® Blood & Tissue Kit, QIAGEN) and used for the HUMARA Assay. This assay was performed by colleagues at the department. A male wildtype cell line and the primary c705delG fibroblasts were also tested.
The results of HUMARA Assay (see Appendix 9.1.), showed that the digestion with the enzyme Hpa II worked and confirmed the presence of monoclonal cells since only one band of each clone after digestion could be observed. In contrast in male control cells only one band was visible which disappears after digestion, while the primary fibroblast cell line shows two bands before and after digestion, which indicate polyclonal origin.

### 7.4.2. Verifying of clonal cells by Immunofluorescence

To verify the aforementioned results, HUMARA Assay clones were studied by immunofluorescence to ascertain whether mutant or wildtype clones were present. Two cell lines, AG21708 wildtype MeCP2 and GM21921 MeCP2-deficient cells, were used as a control. IF has confirmed the presence of one wildtype clone (MeCP2 positive) and two mutant clones (MeCP2 negative).
The following pictures [Figure 9 + 10] were taken using a fluorescence microscope (Leica DMRB RB Microscope Fluorescence DM RB Type 301-371.010) at 20x magnification:

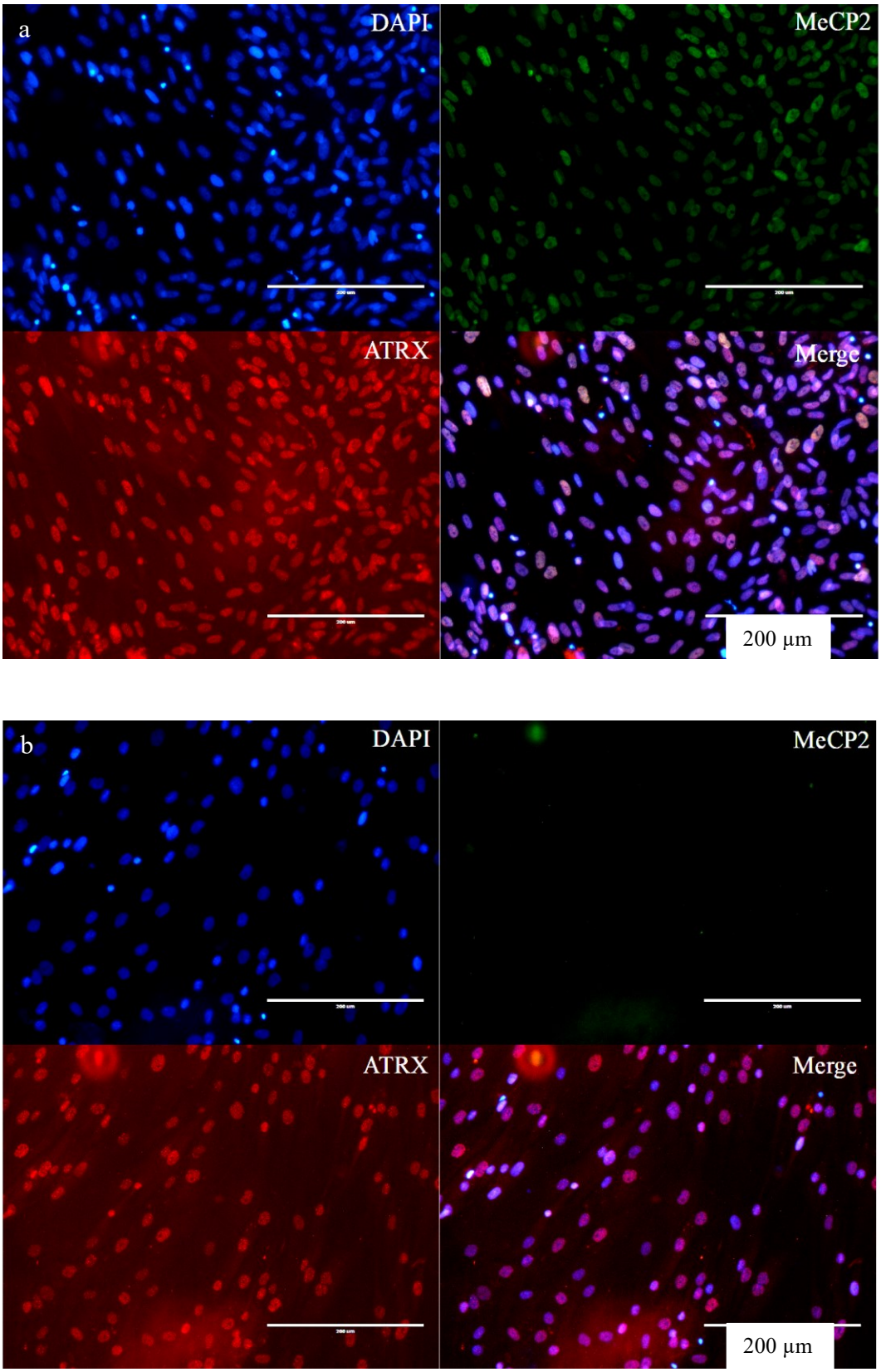


***Figure 9 a | b.*** *Immunofluorescence images from two control cell lines at 20x magnification.* ***a*** *| AG21708 control cells expressing MeCP2.* ***b*** *| GM21921 MeCP2 deficient cells. Images show the staining with DAPI (blue), MeCP2 (green), ATRX (red) and the merge of all the single images.*

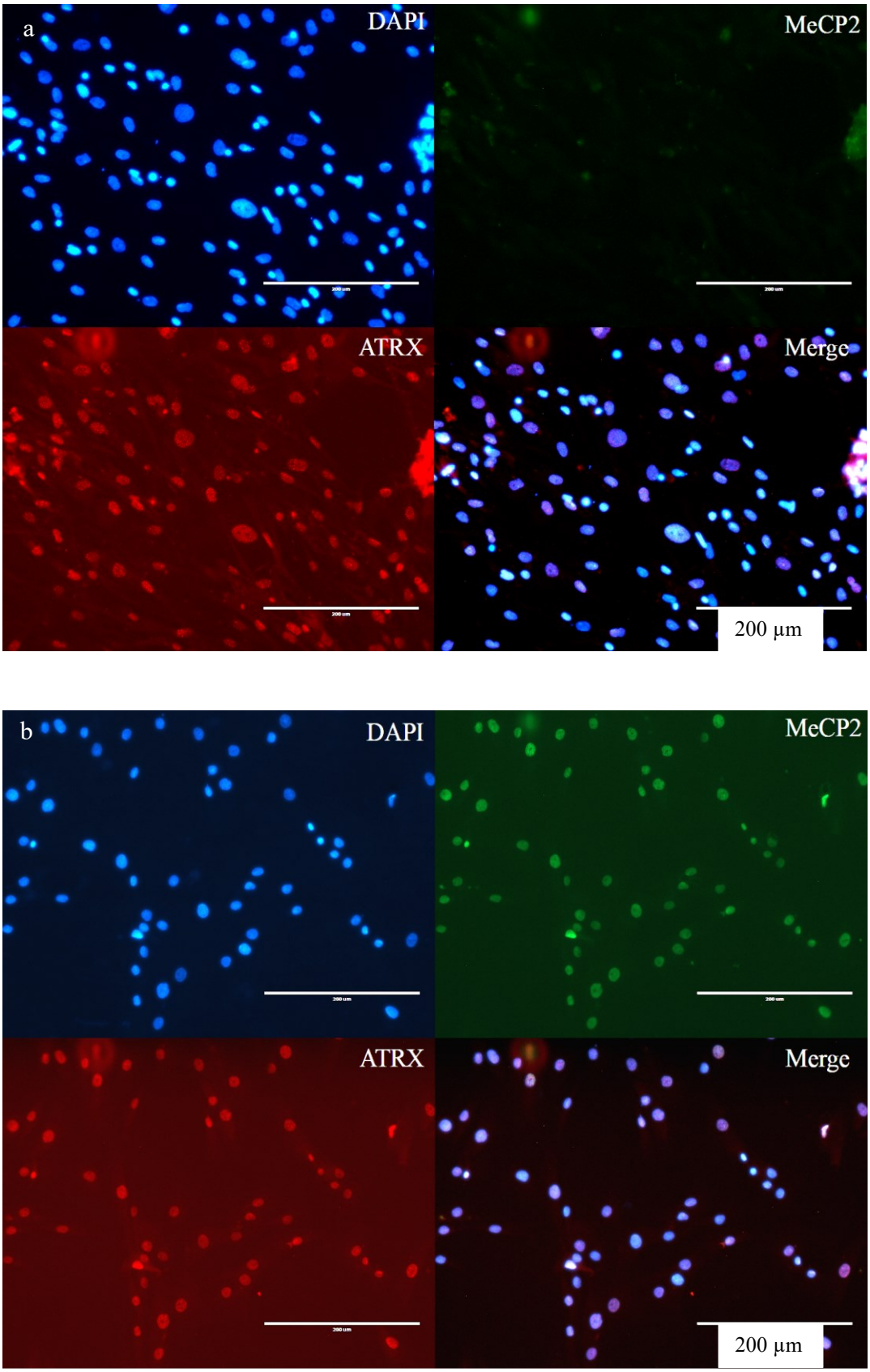


***Figure 10 a | b.*** *Immunofluorescence images from obtained clones at 20x magnification.* ***a*** *| Clone with MeCP2 deficient cells (mutant).* ***b*** *| Clone expressing MeCP2 positive cells (wildtype). Images show the staining with DAPI (blue), MeCP2 (green), ATRX (red) and the merge of all the single images.*

## 7.5. Determination of the genotype of the T158M cell line

Initial attempts with primary fibroblasts showed that the MeCP2 XP antibody, as expected, worked for c705delG but not for T158M [Figure 11]. This occurs because the latter mutation does not lead to a complete degradation of the protein and the antibody probably does not bind in the area of the mutation. Thus, clonality could not be determined by IF. While the MeCP2 XP antibody can differentiate between wildtype and c705delG mutant cells, this is not the case for T158M as only positive cells, even mutated ones are stained.

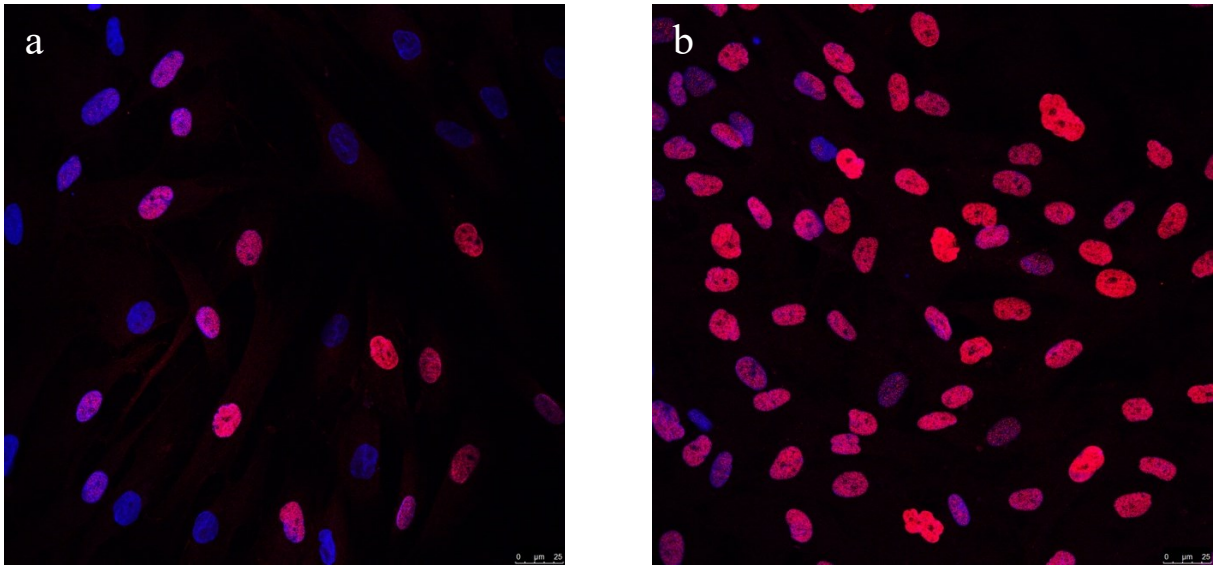


***Figure 11 a | b.*** *Cell lines incubated with the MeCP2 XP antibody at 20x magnification.* ***a*** *| Cells carrying the mutation c705delG can be differentiated in either wildtype or mutant cells using the MeCP2 XP antibody.* ***b*** *| Cells carrying the mutation T158M cannot be differentiated into wildtype and mutant cells as all cells seem to be MeCP2 positive.*

### 7.5.1. Confirmation of the presence of MeCP2 positive cells by sequencing

After RNA had been isolated from clones (RNeasy Plus Mini Kit, QIAGEN) it was reverse-transcribed into cDNA (iScript gDNA Clear cDNA Synthesis Kit, BIO-RAD). PCR was performed with clones of cell line T158M [Figure 12].

Primer pair that worked best was:

Forward Primer: MeCP2_RT_Ex3_F

5'-AGCTTAAGCAAAGGAAATCTGGCC-3'

Reverse Primer: MeCP2_RT_Ex4_R

5'-GGAAGCTCCTTGTCAAGATGCCT-3'

Three different Master Mixes were used:

1. Dream Taq Master Mix, Thermo Scientific
2. Red HS Taq Master Mix, Biozym
3. TAKARA LA Taq Master Mix, Takara

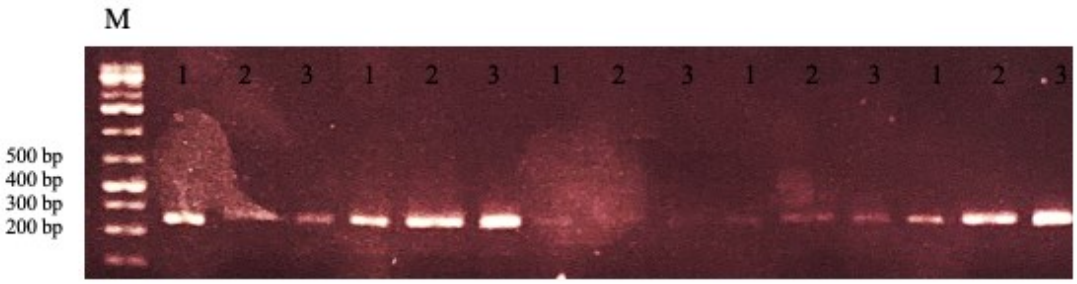


***Figure 12.*** *PCR that was performed with the cells of the mutation T158M. Among all three, the TAKARA Master Mix showed the strongest bands.*

PCR products with strongest bands were used for sequencing by colleagues. Sequencing results proved that all clones were MeCP2 positive cells as no mutation was detected [Figure 13]. Normally, MeCP2 negative cells of T158M result in a C to T transition.

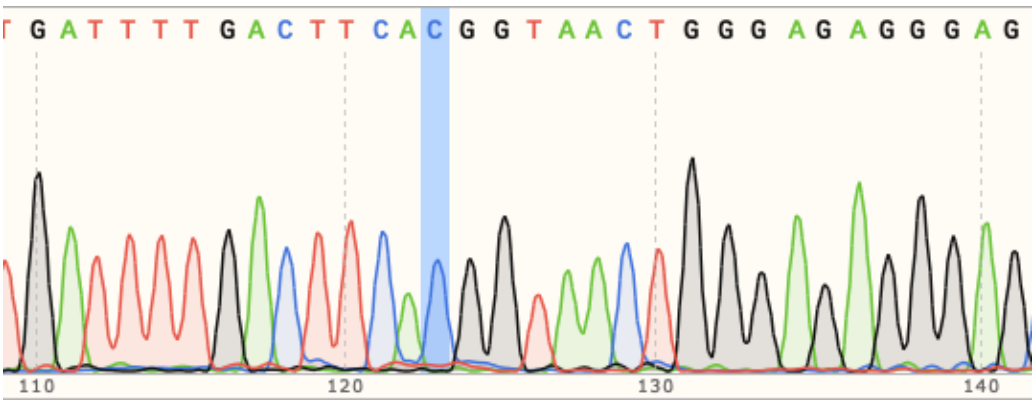


***Figure 13.*** *Results of sequencing. Showing the presence of MeCP2 positive cells because no C to T transition was detected (see blue marking).*

## 7.6. Acetylation status of RETT monoclonal cells

First, we confirmed that MeCP2 protein is expressed in wildtype clonal cell lines derived from a female RTT patient carrying a 705delG mutation and is lacking in mutant clonal cell lines. MeCP2 truncation mutations are known to cause H3/H4 hyperactylation (Wan et al., 2001). Therefore, we set out to determine the status of histone acetylation in eight monoclonal cell lines by immunoblotting with an antibody directed against acetylated histone H3 at Lys9 (H3K9). We found a significant hyperacetylation of the histone H3K9 in

monoclonal cell lines expressing the mutated MECP2 allele compared to cell lines expressing the wild-type MECP2 allele [Figure 14 a+b]. These results are consistent with previous work (Shahbazian et al., 2002; Wan et al., 2001) and confirms that this cellular model can recapitulate the aspects of this genetic disease at least partially.

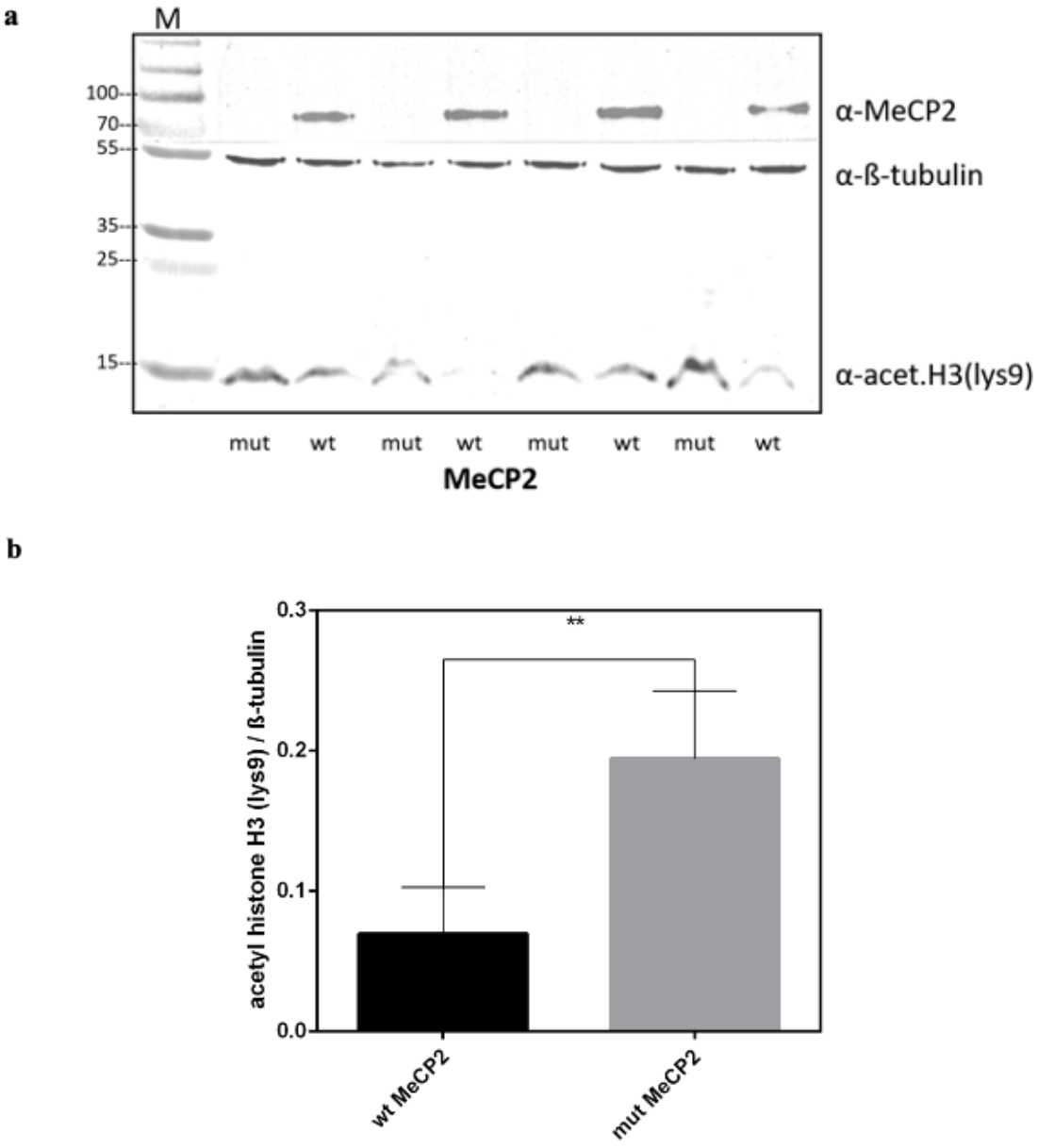


***Figure 14* a | b.** *Analysis of acetylation status in RTT patient (c705delG) expressing wild-type and mutated allele.* ***a****| 100µg of protein lysate of each cell line expressing wild-type (wt, n=4) and mutated (mut, n=4) allele were immunoblotted and probed with antibody against acetylated histone H3 (lys9). Anti-ß-tubulin was used as a loading control to show equal loading amounts of the protein. Anti-MeCP2 was used to show monoclonality of cells derived from patient with Rett syndrome (705delG).* ***b****| The semi-quantitative densitometric analysis of western blot generated signals confirms the histone H3 (lys9) hyperacetylation in mutant cells.*

# 8. Discussion

## 8.1. Single cell isolation

MeCP2 is a chromosomal protein that belongs to the MBD protein family. It is implicated in chromatin remodeling and transcriptional regulation (Jin et al., 2017). Mutations in the MeCP2 gene, which occur on the X chromosome, have been shown to be the prime cause for RTT. A random X chromosome inactivation results in a mix of wild type and mutant cells in the same individuals. In these girls, there is a mosaic of cells that contain the functional MeCP2 protein and cells that do not function properly (Renthal et al., 2018).

While treatment of RTT is currently limited to symptomatic relief and physical therapy, ongoing research is aimed to cure this disease (Kaufmann et al., 2016, Steinkellner et al., 2019;). In order to achieve this goal, developing cell models of wild type and RTT-afflicted cells is of utmost importance.

Therefore, the purpose of this thesis was to describe different methods for single cell isolation of dermal fibroblast cell lines derived from RTT patients with the overall goal to obtain monoclonal wildtype and mutant MeCP2 cells, which are reported here.

The first part of this work is focused on different methods of single cell isolation and the interest focus on a single MeCP2 cell. Because there are many methods for isolating single cells and obtaining MeCP2 positive and negative clones, three methods, FC, limiting dilution and QIAscout™ were selected. These methods all possess their advantages and drawbacks.

While limiting dilution cloning is easy to perform due to its simple handling without a need for specialized equipment or technique, FC for single cell isolation was also employed. This method employs single cell picking that is almost entirely automated thereby saving time and obtaining more reliable results. However, although clones were available with each of these methods, only three clones were obtained out of two FC seeded 96-well plates.

Automatic pipetting by a machine yields a higher chance of isolating single cells. Nevertheless, there were less monoclonal cells than expected, and cells were not growing properly in general, hence the use of this method was discontinued. Due to the availability of

other existing methods such as limiting dilution and QIAscout™ as well as the high costs of a FC machine, the single cell isolation with FC was not repeated again.

The third method used was the QIAscout™. This method is very labor–intensive and cells have to be targeted and picked manually, so any cells of interest can be selected. To date no research was published about the QIAscout™.

The process of picking single cells and cultivating them over a period of approximately six weeks, requires a contamination-free sterile work environment.
The inverted microscope that was used for the QIAscout™, was not located in a sterile environment, however. It had to be placed under the laminar air flow, after being sterilized. Four weeks after single cell picking at first seeding, QIAscout™ well plates showed contamination which brought up the question with what and how were they contaminated. Contamination could have happened during the single cell picking itself, while the cells were cultivated or even at the change of medium over the weeks. Cleaning procedure of magnetic wand and release needle was modified and included: cleaning with 70% ethanol and let it air dry, cleaning with sterile water and agents containing of 3-5% hypochloride. The manufacturer has also recommended keeping the array always closed and it was also suggested to open the lid only for transfer of the pierced raft. This cleaning procedure was then used for all other seedings that were performed with QIAscout™. When these instructions were followed no more contamination was observed in the following seedings.

## 8.2. Treatment of single cells

When it comes to the treatment of the single cell clones, various medium preparations were used. These include culture medium (DMEM), conditioned medium and treatment with amniopan (a medium for the cultivation of human fetal cells from amniotic fluid and chorionic villus sampling (PAN-Biotech)). Immortalized cells were transfected with hTERT and selected with an antibiotic G418 disulfate salt solution.

Immortalized cells transfected with the plasmid pCl neo-hEST2 via electroporation and selection using G418 disulfate salt solution did not lead to the expected results. Although some clones were present, most of them were only wildtype MeCP2 cells. It was subsequently investigated whether the G418 treatment was resulting in MeCP2 read-through and therefore

positive immunofluorescence staining in MeCP2 mutant cells. We treated non-transfected dermal fibroblast cells with G418 together with a negative control. The results showed that abundance of wild type clones occurs independently of G418 treatment.

In another experiment, c705delG cells were cultured in amniopan. This did not lead to a better outcome and additionally resulted in slower growth and even senescent cells. In summary, non-immortalized cells which were treated with culture- and conditioned medium, preserved wildtype and mutant MeCP2 clones.

Therefore, the treatment with the plasmid seems to be a disruptive factor in cell cloning presumably due to additional stress induction. The best result occurred with non-immortalized cells, as these generated two mutant MeCP2 positive clones. T158M cells were getting confluent very quickly while the possible immortalized variant of this cell line did not grow properly anymore in later seedings. This proves that the treatment with this plasmid lead to stress induction and therefore a disruption of cell growth. This brings one to a once conclusion that the plasmid pCl neo-hEST2 was not appropriate and another plasmid could be a better fit. Alternatively, the concentration of G418 could be reduced after successful selection. The treatment with amniopan has resulted in a slower cell growth as well as an inability to achieve confluency.
In conclusion, cells reached best confluency when cultured with culture medium and conditioned medium.

In addition, although there was a high number of MeCP2 positive cells, there were almost no MeCP2 negative cells. This indicates that the balance has shifted strongly towards wildtype MeCP2 due to the transfection with the plasmid. That is why no mutant clone was available after attempted immortalization of the cells which showed that once again that hTERT transfection was not efficient in obtaining single cell clones for further experiments.

## 8.3. Identification of clones

After single cells were picked and treated with different medium, preserved clones of both cell lines had to be analyzed by IF. First primary fibroblasts itself were examined. It was confirmed that the MeCP2 XP antibody did not work, as expected, on the T158M cell line and therefore could not distinguish between MeCP2 positive and negative cells, which did not make it possible to determine the type of clones obtained.

Therefore, T158M clones were characterized by sequencing. Genotyping followed by sequencing confirmed the presence of monoclonal MeCP2 positive cells.

## 8.4. Hyperacetylation in RTT

MeCP2's transcriptional activity includes the compaction and altering of chromatin (Nectoux et al., 2010). After binding to the methylated CpG in the target DNA, MeCP2 recruits the co-repressor Sin3A and histone deacetylase into a complex. The complex deacetylates the tails of histones H3 and H4 in the nucleosomes which leads to compaction of chromatin and is responsible for the silencing of gene expression (Webb & Latif, 2001). Therefore, the status of histone acetylation changes in eight monoclonal cell lines was determined by immunoblotting with an antibody directed against acetylated histone H3 at Lys9 (H3K9). This showed a significant hyperacetylation of the histone H3K9 in monoclonal cell lines expressing the mutated *MECP2* allele compared to cell lines expressing the wild type *MECP2* counterpart. Silencing can therefore potentially be also reversed by inhibiting the histone deacetylase in further experiments (Webb & Latif, 2001).

## 8.5. Conclusion

In conclusion, more research is needed to attain the goal of monoclonal MeCP2 cells as well as to achieve better results in cloning and avoiding a possible shift in the balance towards wild type MeCP2 cells. Optimization of medium conditions as well as the use of a proper plasmid could lead to better results in single cell cloning from dermal fibroblasts of RTT patients.

The possibility of obtaining clones of both, MeCP2 positive and negative cells, would enable further research of the MeCP2 gene such as further analysis of MeCP2 and its methylation, for instance. A further aim would be to take a closer look at the clones on RNA and protein levels. At the protein level, clones could be analyzed by immunofluorescence staining of certain proteins whose expression is altered in RTT, for example Histone H3 and H4 or ATRX, and verifying these findings by western blots (Shahbazian et al., 2002). At the RNA level, specific target genes could be assayed using real-time PCR (Chahrour & Zoghbi, 2007).

The obtained mutant clones could also serve as a cell model for high throughput screening (Jain & Heutink, 2010) or for the verification of TAT-MeCP2's functional effect on the cells in protein replacement therapy (Steinkellner et al., 2019).

# 9. Appendix

## 9.1. Results of the HUMARA Assay before and after digestion

### 9.1.1. Clone A

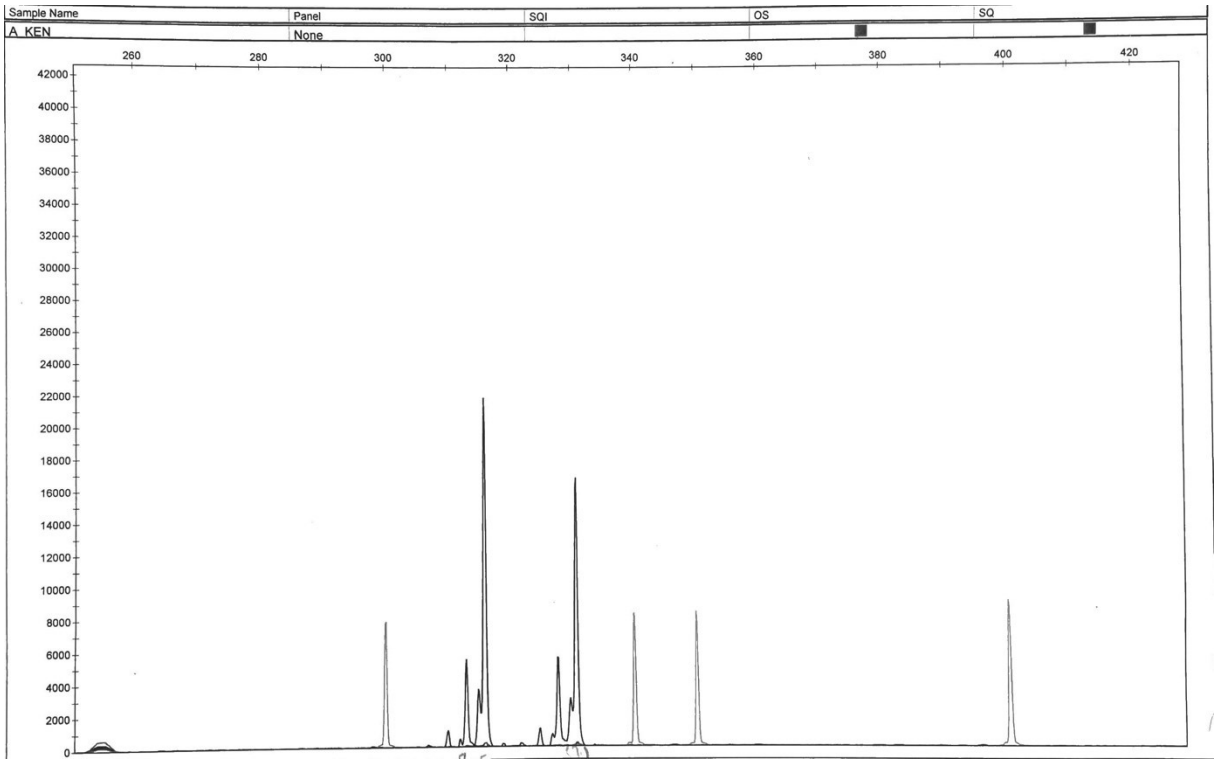


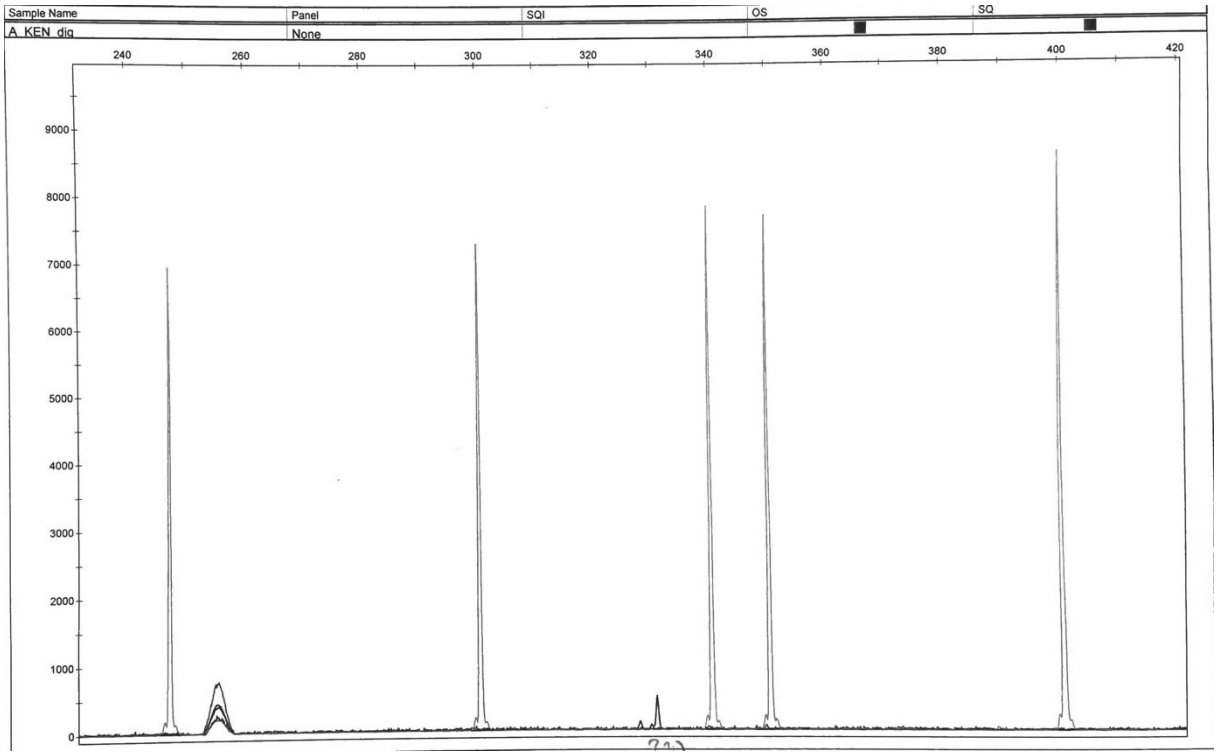

9.1.2. Clone B

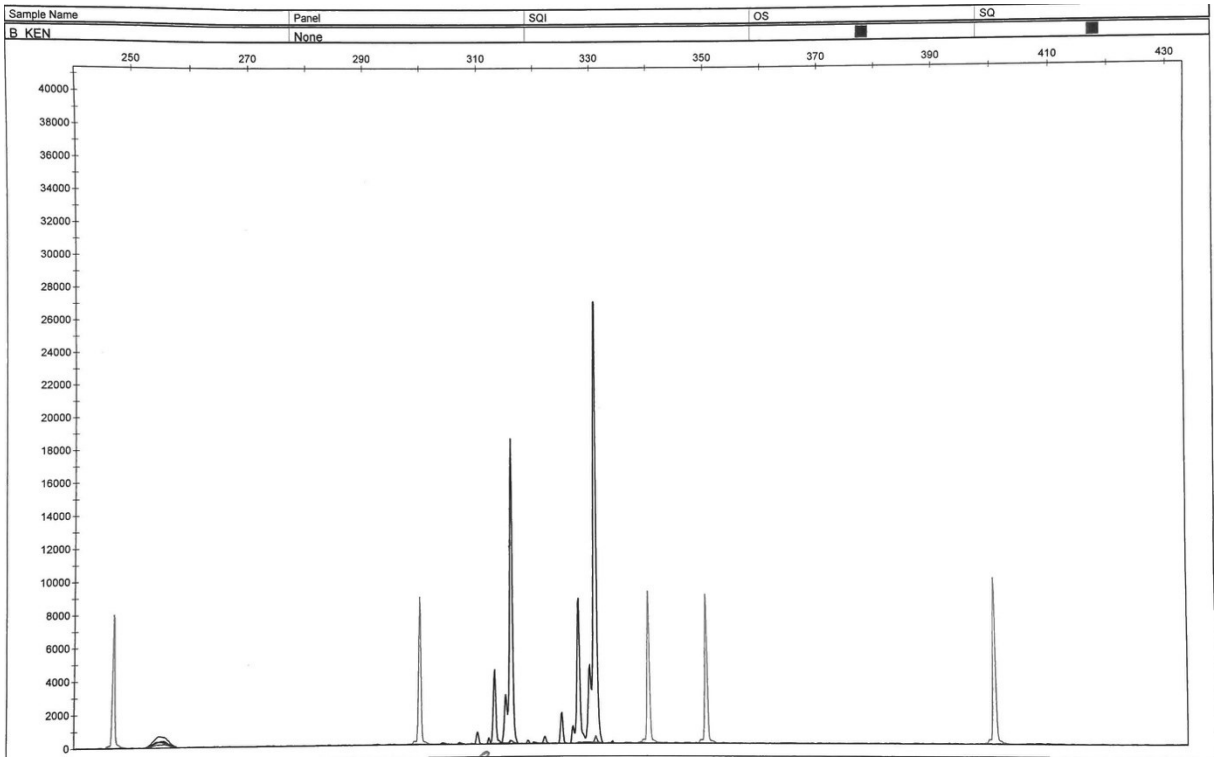
Sample Name
Panel
SQI
OS
SQ
B_KEN
None
250
270
290
310
330
350
370
390
410
430
40000
38000
36000
34000
32000
30000
28000
26000
24000
22000
20000
18000
16000
14000
12000
10000
8000
6000
4000
2000
0

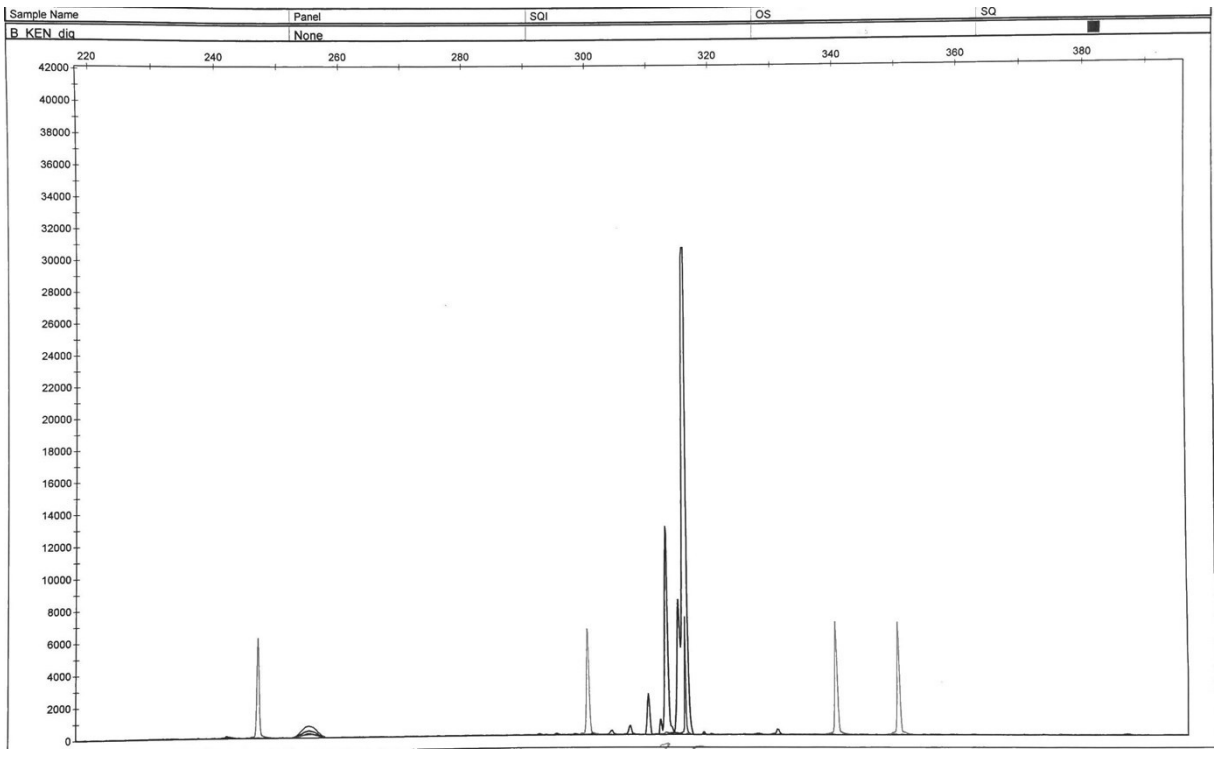
Sample Name
Panel
SQI
OS
SQ
B_KEN_dig
None
220
240
260
280
300
320
340
360
380
42000
40000
38000
36000
34000
32000
30000
28000
26000
24000
22000
20000
18000
16000
14000
12000
10000
8000
6000
4000
2000
0

### 9.1.3. Clone C

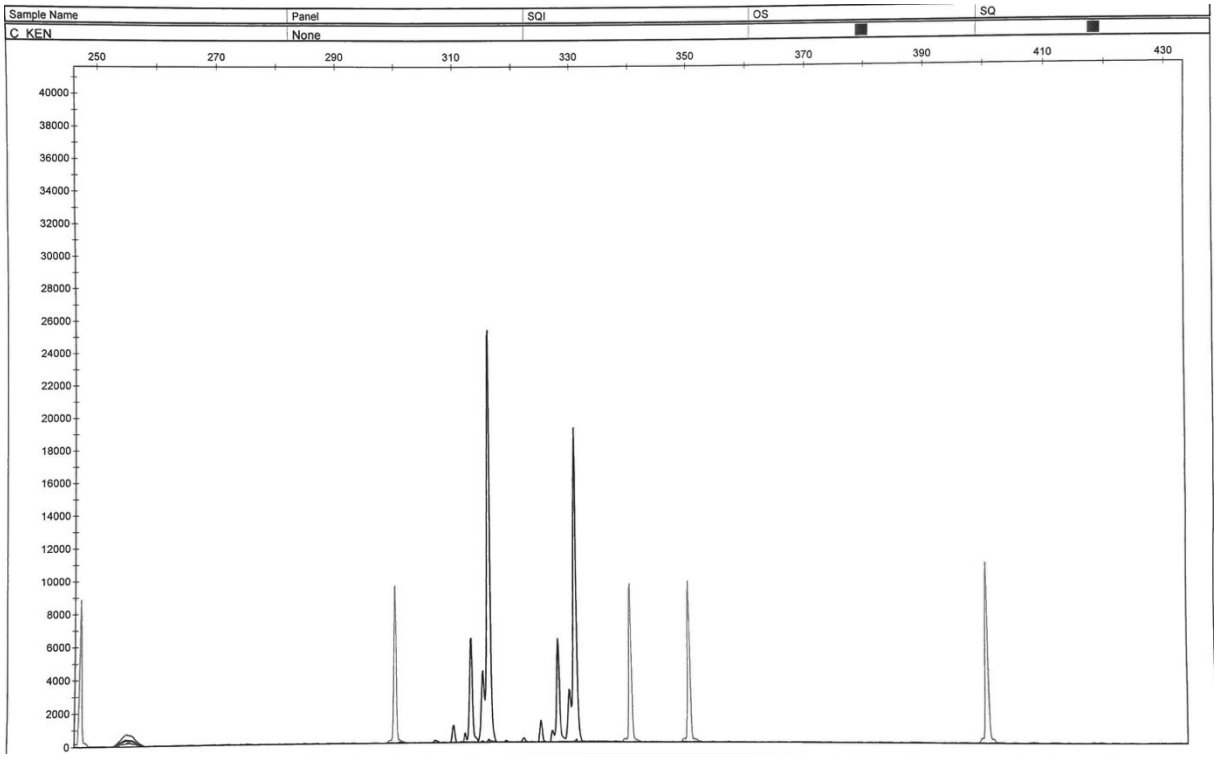
Sample Name
Panel
SQI
OS
SQ
C_KEN
None
250
270
290
310
330
350
370
390
410
430
40000
38000
36000
34000
32000
30000
28000
26000
24000
22000
20000
18000
16000
14000
12000
10000
8000
6000
4000
2000
0

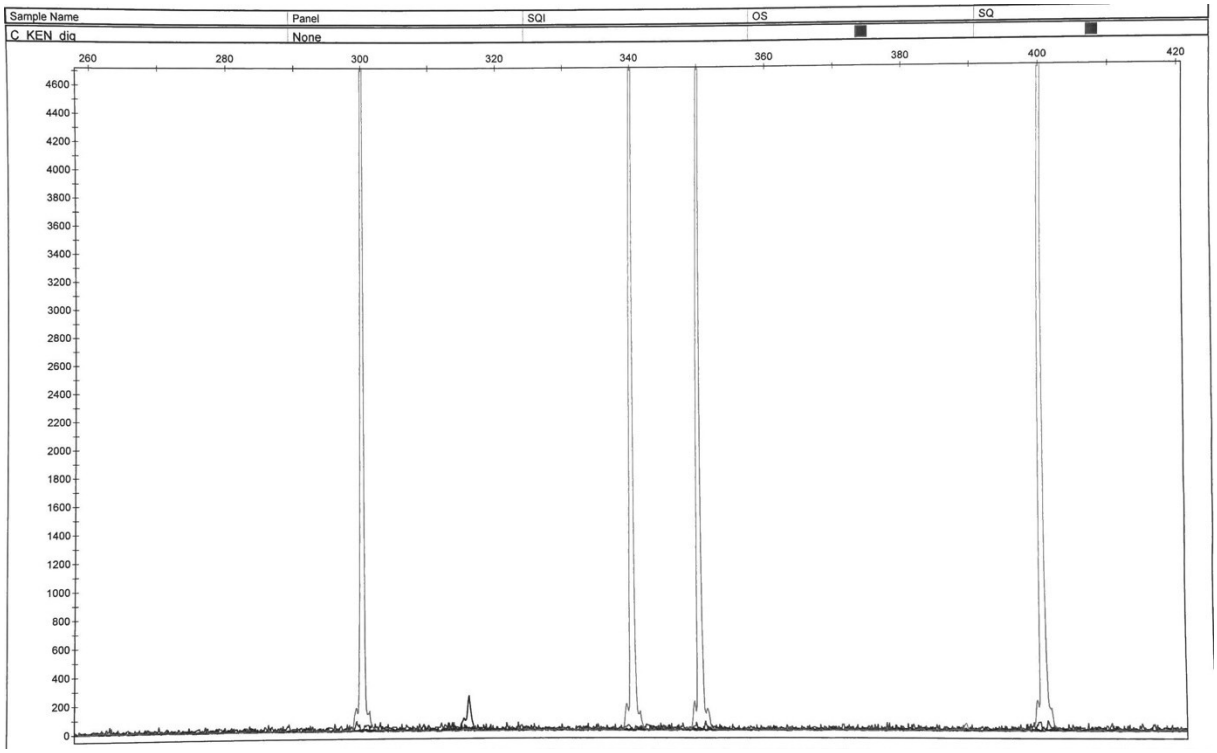
Sample Name
Panel
SQI
OS
SQ
C_KEN_dig
None
260
280
300
320
340
360
380
400
420
4600
4400
4200
4000
3800
3600
3400
3200
3000
2800
2600
2400
2200
2000
1800
1600
1400
1200
1000
800
600
400
200
0

9.1.4. c705delG

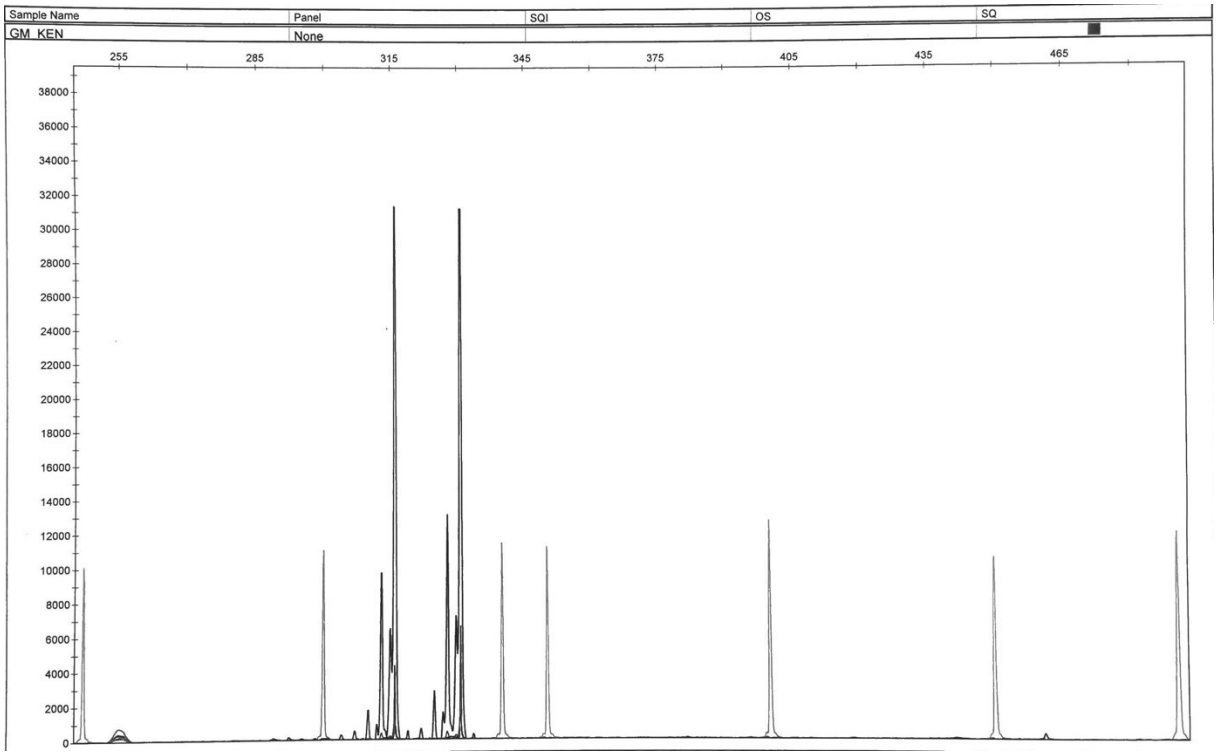


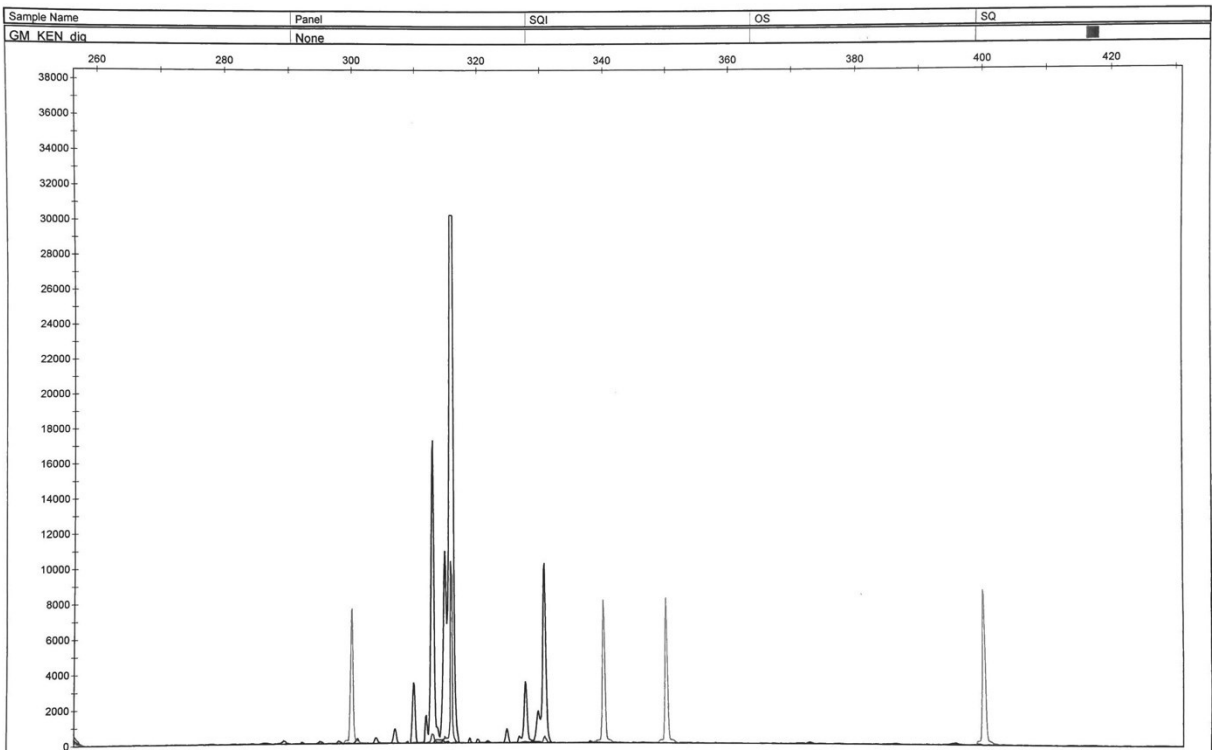

9.1.5. Male control cells

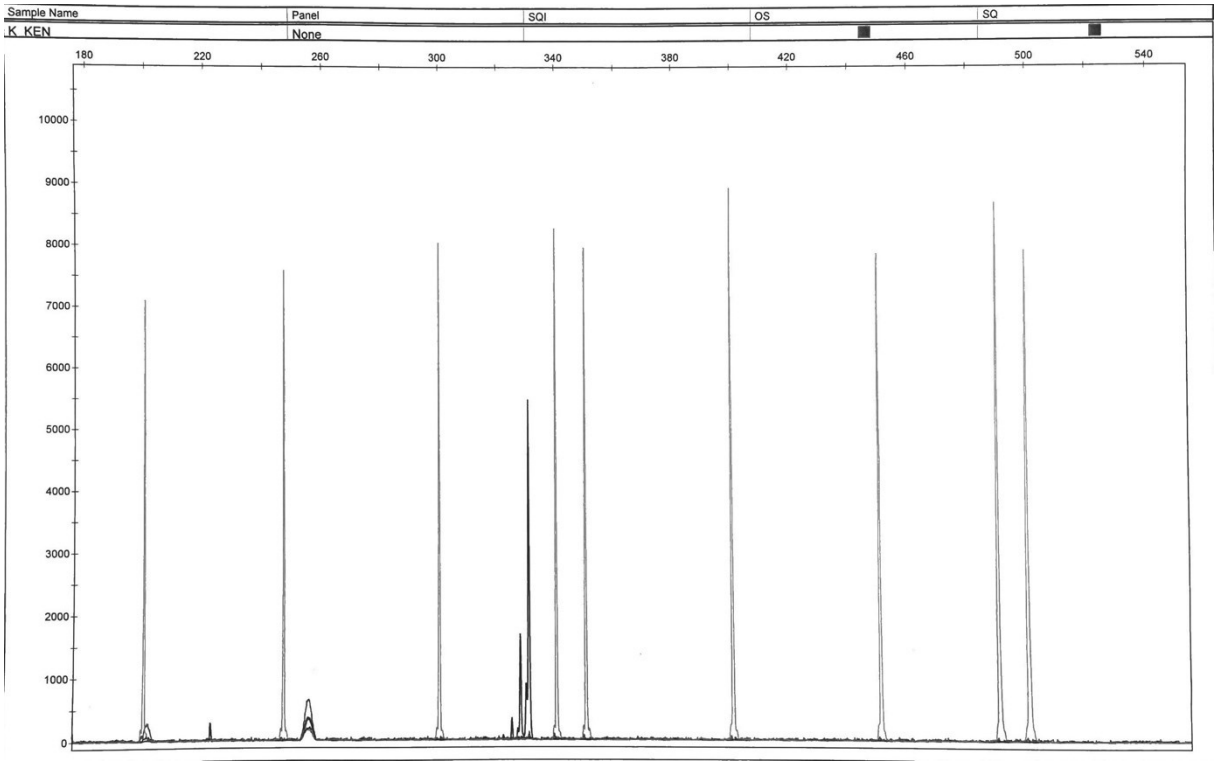


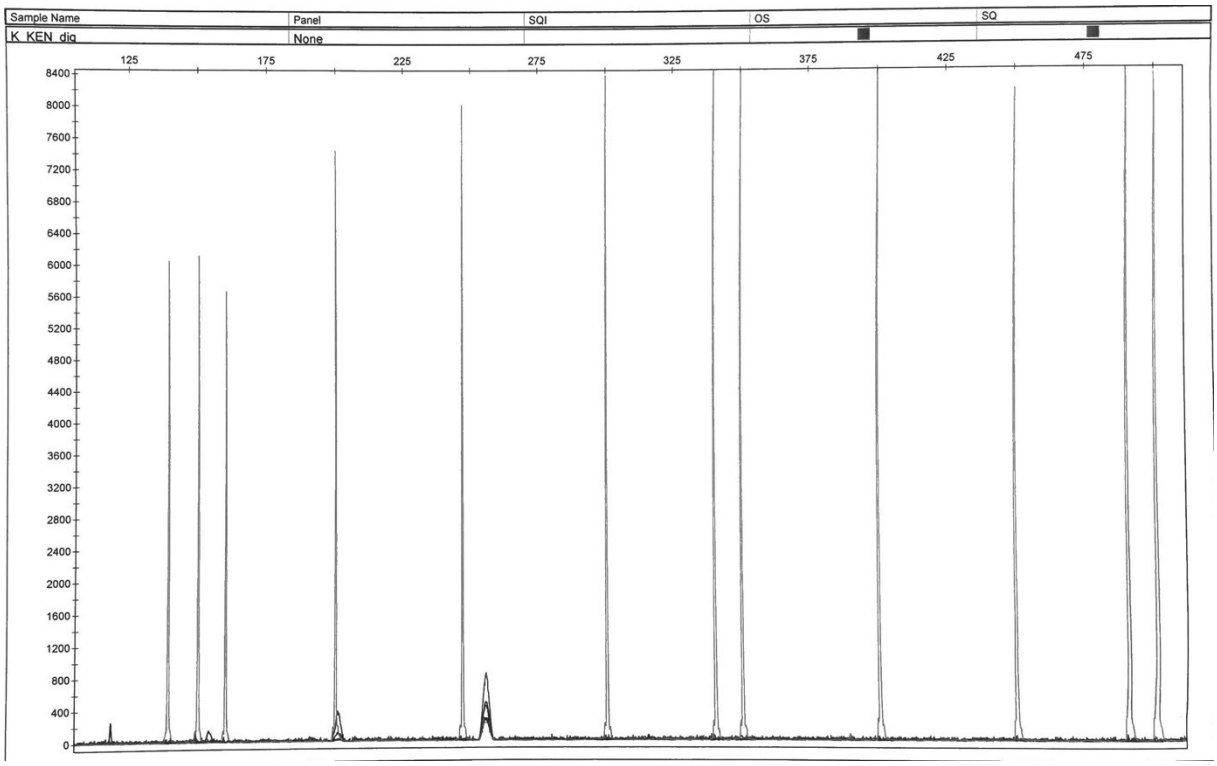

# 10. References


Buyse, I. M., Fang, P., Hoon, K. T., Amir, R. E., Zoghbi, H. Y., & Roa, B. B. (2000). Diagnostic testing for Rett syndrome by DHPLC and direct sequencing analysis of the MECP2 gene: Identification of several novel mutations and polymorphisms. *American Journal of Human Genetics*. https://doi.org/10.1086/316913

Chahrour, M., Sung, Y. J., Shaw, C., Zhou, X., Wong, S. T. C., Qin, J., & Zoghbi, H. Y. (2008). MeCP2, a key contributor to neurological disease, activates and represses transcription. *Science*. https://doi.org/10.1126/science.1153252

Chahrour, M., & Zoghbi, H. Y. (2007). The Story of Rett Syndrome: From Clinic to Neurobiology. In *Neuron*. https://doi.org/10.1016/j.neuron.2007.10.001

Chapleau, C. A., Lane, J., Pozzo-Miller, L., & Percy, A. K. (2013). Evaluation of current pharmacological treatment options in the management of Rett syndrome: from the present to future therapeutic alternatives. In *Current clinical pharmacology*. https://doi.org/10.2174/15748847113086660069

Ehrhart, F., Coort, S. L. M., Cirillo, E., Smeets, E., Evelo, C. T., & Curfs, L. M. G. (2016). Rett syndrome - Biological pathways leading from MECP2 to disorder phenotypes. In *Orphanet Journal of Rare Diseases*. https://doi.org/10.1186/s13023-016-0545-5

*GM07982*. (n.d.). Retrieved May 22, 2020, from https://www.coriell.org/0/Sections/Search/Sample_Detail.aspx?Ref=GM07982&Product=CC

*GM17880*. (n.d.). Retrieved May 22, 2020, from https://www.coriell.org/0/Sections/Search/Sample_Detail.aspx?Ref=GM17880&Product=CC

Gross, A., Schoendube, J., Zimmermann, S., Steeb, M., Zengerle, R., & Koltay, P. (2015). Technologies for single-cell isolation. In *International Journal of Molecular Sciences*. https://doi.org/10.3390/ijms160816897

Hu, P., Zhang, W., Xin, H., & Deng, G. (2016). Single cell isolation and analysis. In *Frontiers in Cell and Developmental Biology*. https://doi.org/10.3389/fcell.2016.00116

*Improving Clone Isolation and Screening In Hybridoma Cells – Moving away from Limiting Dilution - Cell Culture Dish*. (n.d.). Retrieved June 26, 2020, from https://cellculturedish.com/improving-clone-isolation-and-screening-in-hybridoma-cells-moving-away-from-limiting-dilution/

Jain, S., & Heutink, P. (2010). From single genes to gene networks: High-throughput-high-content screening for neurological disease. In *Neuron*. https://doi.org/10.1016/j.neuron.2010.10.010

Jin, X. R., Chen, X. S., & Xiao, L. (2017). MeCP2 deficiency in neuroglia: New progress in the pathogenesis of rett syndrome. In *Frontiers in Molecular Neuroscience*. https://doi.org/10.3389/fnmol.2017.00316

Katz, D. M., Bird, A., Coenraads, M., Gray, S. J., Menon, D. U., Philpot, B. D., & Tarquinio, D. C. (2016). Rett Syndrome: Crossing the Threshold to Clinical Translation. In *Trends in Neurosciences*. https://doi.org/10.1016/j.tins.2015.12.008

Kaufmann, W. E., Stallworth, J. L., Everman, D. B., & Skinner, S. A. (2016).

Neurobiologically-based treatments in Rett syndrome: opportunities and challenges. In *Expert Opinion on Orphan Drugs*. https://doi.org/10.1080/21678707.2016.1229181

Kyle, S. M., Vashi, N., & Justice, M. J. (2018). Rett syndrome: A neurological disorder with metabolic components. In *Open Biology*. https://doi.org/10.1098/rsob.170216

Leonard, H., Cobb, S., & Downs, J. (2016). Clinical and biological progress over 50 years in Rett syndrome. In *Nature Reviews Neurology*. https://doi.org/10.1038/nrneurol.2016.186

Liyanage, V. R. B., & Rastegar, M. (2014). Rett syndrome and MeCP2. *NeuroMolecular Medicine*. https://doi.org/10.1007/s12017-014-8295-9

Luikenhuis, S., Giacometti, E., Beard, C. F., & Jaenisch, R. (2004). Expression of MeCP2 in postmitotic neurons rescues Rett syndrome in mice. *Proceedings of the National Academy of Sciences of the United States of America*. https://doi.org/10.1073/pnas.0401626101

Mari, F., Caselli, R., Russo, S., Cogliati, F., Ariani, F., Longo, I., Bruttini, M., Meloni, I., Pescucci, C., Schurfeld, K., Toti, P., Tassini, M., Larizza, L., Hayek, G., Zappella, M., & Reniere, A. (2005). Germline mosaicism in Rett syndrome identified by prenatal diagnosis. *Clinical Genetics*. https://doi.org/10.1111/j.1399-0004.2005.00397.x

McCauley, M. D., Wang, T., Mike, E., Herrera, J., Beavers, D. L., Huang, T. W., Ward, C. S., Skinner, S., Percy, A. K., Glaze, D. G., Wehrens, X. H. T., & Neul, J. L. (2011). Rett syndrome: Pathogenesis of lethal cardiac arrhythmias in Mecp2 mutant mice: Implication for therapy in Rett syndrome. *Science Translational Medicine*. https://doi.org/10.1126/scitranslmed.3002982

McKinnon, K. M. (2018). Flow cytometry: An overview. *Current Protocols in Immunology*. https://doi.org/10.1002/cpim.40

Nectoux, J., Fichou, Y., Rosas-Vargas, H., Cagnard, N., Bahi-Buisson, N., Nusbaum, P., Letourneur, F., Chelly, J., & Bienvenu, T. (2010). Cell cloning-based transcriptome analysis in Rett patients: Relevance to the pathogenesis of Rett syndrome of new human MeCP2 target genes. *Journal of Cellular and Molecular Medicine*. https://doi.org/10.1111/j.1582-4934.2010.01107.x

*Österreichische Rett-Syndrom Gesellschaft*. (n.d.). Retrieved June 6, 2020, from www.rett-syndrom.at

*QIAscout User Manual - QIAGEN*. (n.d.). Retrieved October 15, 2020, from https://www.qiagen.com/us/resources/resourcedetail?id=f992cbfc-ebcd-4bc3-8440-f93b5995e944&lang=en

Renthal, W., Boxer, L. D., Hrvatin, S., Li, E., Silberfeld, A., Nagy, M. A., Griffith, E. C., Vierbuchen, T., & Greenberg, M. E. (2018). Characterization of human mosaic Rett syndrome brain tissue by single-nucleus RNA sequencing. *Nature Neuroscience*. https://doi.org/10.1038/s41593-018-0270-6

*Rett syndrome - Wikipedia*. (n.d.). Retrieved June 8, 2020, from https://en.wikipedia.org/wiki/Rett_syndrome

Ross, P. D., Guy, J., Selfridge, J., Kamal, B., Bahey, N., Elizabeth Tanner, K., Gillingwater, T. H., Jones, R. A., Loughrey, C. M., McCarroll, C. S., Bailey, M. E. S., Bird, A., & Cobb, S. (2016). Exclusive expression of MeCP2 in the nervous system distinguishes between brain and peripheral Rett syndrome-like phenotypes. *Human Molecular Genetics*. https://doi.org/10.1093/hmg/ddw269

Shah, R. R., & Bird, A. P. (2017). MeCP2 mutations: Progress towards understanding and treating Rett syndrome. In *Genome Medicine*. https://doi.org/10.1186/s13073-017-0411-7

Shahbazian, M. D., Young, J. I., Yuva-Paylor, L. A., Spencer, C. M., Antalffy, B. A., Noebels, J. L., Armstrong, D. L., Paylor, R., & Zoghbi, H. Y. (2002). Mice with truncated MeCP2 recapitulate many Rett syndrome features and display hyperacetylation of histone H3. *Neuron*. https://doi.org/10.1016/S0896-6273(02)00768-7

Shahbazian, M. D., & Zoghbi, H. Y. (2001). Molecular genetics of Rett syndrome and clinical spectrum of MECP2 mutations. In *Current Opinion in Neurology*. https://doi.org/10.1097/00019052-200104000-00006

*Single Cell Isolation Trends: Technologies, Limitations & Applications | Technology Networks*. (n.d.). Retrieved May 16, 2020, from https://www.technologynetworks.com/cell-science/articles/single-cell-isolation-trends-technologies-limitations-applications-289361

Smeets, E. E. J., Pelc, K., & Dan, B. (2012). Rett syndrome. *Molecular Syndromology*. https://doi.org/10.1159/000337637

Steinkellner, H., Schönegger, A., Etzler, J., Kempaiah, P., Huber, A., Hahn, K., Rose, K., Duerr, M., Christodoulou, J., Beribisky, A. V., Neuhaus, W., & Laccone, F. (2019). An electrochemiluminescence based assay for quantitative detection of endogenous and exogenously applied MeCP2 protein variants. *Scientific Reports*. https://doi.org/10.1038/s41598-019-44372-3

Thatcher, K. N., & LaSalle, J. M. (2006). Dynamic changes in histone H3 lysine 9 acetylation localization patterns during neuronal maturation require Mecp2. *Epigenetics*. https://doi.org/10.4161/epi.1.1.2339

*Tissue Culture Techniques: An Introduction - Bernice M. Martin - Google Books*. (n.d.). Retrieved June 26, 2020, from https://books.google.at/books?id=0t99mNNGnUcC&pg=PA143&lpg=PA143&dq=advantages+limited+dilution&source=bl&ots=wZQFuxiFB9&sig=ACfU3U1wJWEslWFEIk4pf6Vjf8NSqXIq7w&hl=de&sa=X&ved=2ahUKEwik0On3oKDqAhVMxoUKHWEYCGkQ6AEwA3oECAkQAQ#v=onepage&q=advantages limited dilution&f=false

Traynor, J., Agarwal, P., Lazzeroni, L., & Francke, U. (2002). Gene expression patterns vary in clonal cell cultures from Rett syndrome females with eight different MECP2 mutations. *BMC Medical Genetics*. https://doi.org/10.1186/1471-2350-3-12

Urdinguio, R. G., Pino, I., Ropero, S., Fraga, M. F., & Esteller, M. (2007). Histone H3 and H4 modification profiles in a Rett syndrome mouse model. *Epigenetics*. https://doi.org/10.4161/epi.2.1.3698

Valihrach, L., Androvic, P., & Kubista, M. (2018). Platforms for single-cell collection and analysis. In *International Journal of Molecular Sciences*. https://doi.org/10.3390/ijms19030807

Wan, M., Zhao, K., Lee, S. S. J., & Francke, U. (2001). MECP2 truncating mutations cause histone H4 hyperacetylation in Rett syndrome. *Human Molecular Genetics*. https://doi.org/10.1093/hmg/10.10.1085

Webb, T., & Latif, F. (2001). Rett syndrome and the MECP2 gene. In *Journal of Medical Genetics*. https://doi.org/10.1136/jmg.38.4.217

*What is Rett Syndrome? | Rettsyndrome.org*. (n.d.). Retrieved June 2, 2020, from https://www.rettsyndrome.org/about-rett-syndrome/what-is-rett-syndrome/

Yu, D., Sakurai, F., & Corey, D. R. (2011). Clonal Rett Syndrome cell lines to test compounds for activation of wild-type MeCP2 expression. *Bioorganic and Medicinal Chemistry Letters*. https://doi.org/10.1016/j.bmcl.2011.07.053

Zhang, Q., Wang, T., Zhou, Q., Zhang, P., Gong, Y., Gou, H., Xu, J., & Ma, B. (2017). Development of a facile droplet-based single-cell isolation platform for cultivation and genomic analysis in microorganisms. *Scientific Reports*, *7*(1), 1–11. https://doi.org/10.1038/srep41192